Appendix IV

Climate Change Effects on Vegetation Distribution, Carbon Stocks, and Fire Regimes in California

James M. Lenihan
Raymond Drapek
Ronald Neilson
USDA Forest Service
Pacific Northwest Research Station
Corvallis, Oregon

and

Dominique Bachelet
Oregon State University
Corvallis, Oregon

Contents

Figures

Tables

Abstract

The objective of this study was to dynamically simulate the response of vegetation distribution, carbon stocks, and fire regimes for the historical climate of California, as well as under two contrasting scenarios of climate change. The results of the simulations for the historical climate compared favorably to independent estimates and observations, but validation of the results was complicated by the model's lack of land use effects. The response to increasing temperatures under both scenarios was characterized by shifts in the relative dominance of needleleaf and broadleaf life forms and by changes in the potential production of trees. The simulated response to changes in precipitation was more complex, involving not only the effect of changes in soil moisture on vegetation productivity, but also changes in tree-grass competition mediated by fire. Because the summer months were warmer and persistently dry under both scenarios, simulated changes in fire behavior and effects were primarily a response to changes in simulated fuels. Total ecosystem carbon increased under both climate scenarios, but the proportion allocated to different carbon pools varied. The results of the simulations underscore the potentially large impact of climate change on California ecosystems, and the need for further use and development of dynamic vegetation models using various ensembles of climate change scenarios.

1. Introduction

California is one of the most climatically and biologically diverse areas in the world. There is more diversity in the state's land forms, climate, ecosystems, and species than in any comparably sized region in the United States (Holland and Keil, 1995). The diversity of landscapes and climates supports a broad range of natural ecosystems ranging from the cool and wet redwood forests of the northwestern bioregion to the hot and dry Mojave and Sonoran deserts (Figure 1; Hickman, 1993). This diversity of habitats sustains a greater level of species diversity and endemism than is found in any other region of the nation. The California flora includes approximately 25% of the flora of the continental United States, and about 25% of the plant species are endemic to the state (Davis et al., 1998).

California's trillion-dollar economy is also unrivaled in the United States (Wilkinson and Rounds, 1998), and the state's natural systems are an important component of its economic activities. California's forests provide 10% of the nation's wood products, livestock grazing ranks second among all agricultural commodities in the state, and more than 55% of the state is used for logging, grazing, or both (Jensen et al., 1993). California's 11 million acres of parks and wilderness areas draw millions of tourists to the state each year, more than any other state except Alaska (California Division of Tourism, 2001). In addition, natural systems provide numerous

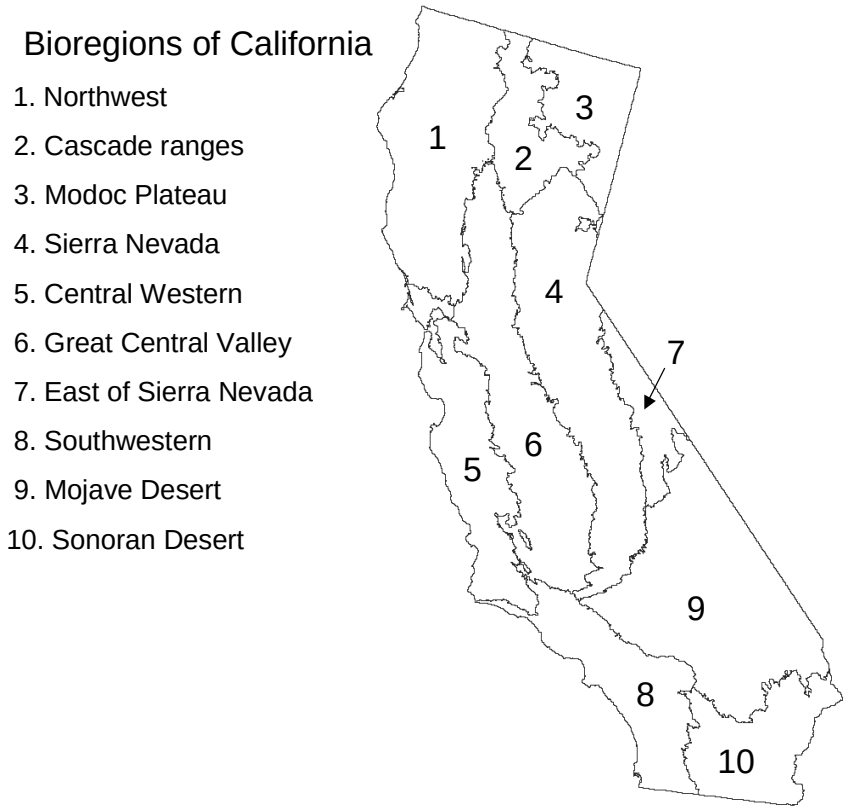

Figure 1. Bioregions of California (Hickman, 1993)

ecosystem services (e.g., water and air purification, mitigation of droughts and floods, cycling and movement of nutrients, and control of potential agricultural pests), which help sustain all sectors of California's economy (Field et al., 1999).

The state's burgeoning population and the consequent impacts on the landscape threaten much of its biological wealth. Throughout the state, natural habitats have been and continue to be altered and fragmented, endangering the state's biological diversity (Barbour et al., 1993). Most of the state's forests have been logged, native oak woodlands are in serious decline, native grasslands have almost completely disappeared, and nearly 90% of the state's wetlands and riparian areas have been severely degraded or destroyed. Even relatively unmanaged natural systems have been significantly altered by introduction of non-native species and by fire suppression (Field et al., 1999). Pervasive human impacts, along with the high level of species endemism in the state, have placed a large number of species at risk of extinction. With 227 species currently listed as endangered or threatened in the state, and many others proposed as candidates for listing, California has the dubious distinction of being the endangered species capital of the nation (U.S. Fish and Wildlife Service, 2001).

In the future, global climate change will increasingly interact with and intensify the pressures of a growing population on California's natural ecosystems. Recent studies show that even gradual and apparently small changes in climate can lead to catastrophic shifts in ecosystems when ecosystem resilience has been compromised by human exploitation (Scheffer et al., 2001). Regional climate studies indicate that, on average, California may experience substantially warmer and wetter winters, somewhat warmer summers, and an enhanced El Niño/Southern Oscillation (ENSO) during the next century (Field et al., 1999; Gutowski et al., 2000). All natural ecosystems, whether managed or unmanaged, will be affected by these changes in climate. It is not possible to accurately predict the response of the natural systems to global climate change through direct experimentation. The physical extent, complexity, and expense of even a single factor experiment for an entire ecosystem are usually prohibitive (Aber et al., 2001). However, analyses of the sensitivity of natural ecosystems to climate change can be made using ecosystem models that integrate information from direct experimentation.

In this study we, used MC1 (Daly et al., 2000; Bachelet et al., 2001b), a state-of-the-art dynamic vegetation model, to investigate the sensitivity of natural ecosystems in California under two different future climate scenarios. MC1 simulates vegetation succession at large spatial extents through time while estimating variability in the carbon budget and responses to episodic events such as drought and fire. Although MC1 does not as yet simulate interactions with land use effects or constraints on ecosystem change imposed by dispersal of propagules, the model has been used to examine the sensitivity of natural ecosystems to global climate change for several national-scale studies, most recently for the U.S. Global Change Research Program's National Assessment of Climate Change Impacts on the United States (Aber et al., 2001; National Assessment Synthesis Team, 2001).

2. Methods

2.1 The Model

MC1 (Daly et al., 2000; Bachelet et al., 2001b) is a dynamic vegetation model (DVM) that simulates life form mixtures and vegetation types; ecosystem fluxes of carbon, nitrogen, and water; and fire disturbance (Lenihan et al., 1998). MC1 is routinely implemented (Bachelet et al., 2000, 2001a; Daly et al., 2000; Aber et al., 2001) on spatial data grids of varying resolution (i.e., grid cell sizes ranging from 30 m^2 to about 2500 km^2) where the model is run separately for each grid cell (i.e., there is no exchange of information across cells). The model reads climate data at a monthly timestep and runs interacting modules that simulate biogeography, biogeochemistry, and fire disturbance.

2.1.1 Biogeography module

The biogeography module simulates the potential life form mixture of evergreen needleleaf, evergreen broadleaf, and deciduous broadleaf trees, along with C3 and C4 grasses. The tree life form mixture is determined at each annual timestep by locating the grid cell on a two-dimensional gradient of annual minimum temperature and growing season precipitation. Life form dominance is arrayed along the minimum temperature gradient from more evergreen needleleaf dominance at relatively low temperatures, to more deciduous broadleaf dominance at intermediate temperatures, to more broadleaf evergreen dominance at relatively high temperatures. The precipitation dimension is used to modulate the relative dominance of deciduous broadleaved trees, which is gradually reduced to zero toward low values of growing season precipitation. Mixtures of C3 versus C4 grasses are determined by reference to their relative potential productivity during the three warmest consecutive months. Potential grass production by life form is simulated as a function of soil temperature using equations from the CENTURY model (Parton et al., 1994). The tree and grass life form mixtures, together with leaf biomass simulated by the biogeochemistry module, are used in a rule base to determine which of 22 possible potential vegetation types occurs at the grid cell each year. The MC1 biogeography rule base was developed using the MAPSS (Neilson, 1995) rule base as a template.

2.1.2 Biogeochemistry module

The biogeochemistry module is a modified version of the CENTURY model (Parton et al., 1994), which simulates plant productivity, organic matter decomposition, and water and nutrient cycling. Plant productivity is constrained by temperature, effective moisture (i.e., a function of soil moisture and potential evapotranspiration), and nutrient availability. The simulated effect of increasing atmospheric carbon dioxide (CO_2) is to increase maximum potential production and to decrease transpiration (thus reducing the constraint of effective moisture on productivity). Trees compete with grasses for soil moisture, light, and nutrients. Competition for water is structured by rooting depth. Trees and grasses compete for soil moisture in the upper soil layers where both life forms are rooted, but the trees with deeper roots have sole access to moisture in deeper soil layers. Grass productivity is constrained by light availability in the understory; the light availability is reduced as a function of tree leaf carbon. Parameterization of the tree and grass growth processes in the model is based on the current life form mixture, which is updated annually by the biogeography module. For example, an increase in annual minimum temperature that shifted the dominance of evergreen needleleaf trees to codominance with evergreen broadleaf trees would trigger an adjustment of tree growth parameters (e.g., the optimum growth temperature) that would, in turn, produce a modified tree growth rate.

2.1.3 Fire disturbance module

The MC1 fire module (Lenihan et al., 1998) simulates the occurrence, behavior, and effects of fire. The module consists of several mechanistic fire behavior and effect functions (Rothermel, 1972; Peterson and Ryan, 1986; van Wagner, 1993; Keane et al., 1997), embedded in a structure that provides two-way interactions with the biogeography and biogeochemistry modules. Live crown structure and fuel loading in several size classes of both dead and live fuels are estimated using life-form-specific allometric functions of the different carbon pools. The moisture content of each dead fuel size class is estimated as a function of antecedent weather conditions averaged over a period of days dependent on size class. The moisture content of each live fuel size class is a function of the soil moisture content to a specific depth in the profile. Fuel moisture and distribution of the total fuel load among different size classes determine potential fire behavior estimated using the Rothermel (1972) fire spread equations.

The rate of fire spread and the intensity of the fire line are the model estimates of fire behavior used to simulate fire occurrence and effects. A fire event is triggered by thresholds of fire spread, fine fuel flammability, and coarse woody fuel moisture (given a constraint of just one fire event per year). The thresholds were calibrated to limit the occurrence of simulated fires to only the most extreme events. Large and severe fires account for a very large fraction of the annual area burned historically (Strauss et al., 1989). These events are also likely to be least constrained by heterogeneities in topography, fuel moisture, and fuel loading that are poorly represented by relatively coarse-scale input data grids (Turner and Romme, 1994).

The direct effect of fire in the model is the consumption and mortality of dead and live vegetation carbon that is removed from (or transferred to) the appropriate carbon pools in the biogeochemistry module. This direct effect is a function of the simulated fraction of the cell burned, fire-line intensity, and tree canopy structure. The fraction of the cell burned depends on the simulated rate of fire spread and the time since the last fire event relative to the current fire return interval simulated for the cell. Higher rates of spread and longer intervals between fires generally produce more extensive fire events in the model. Live carbon mortality and consumption within the burned area are functions of fire-line intensity and the tree canopy structure (i.e., crown height, crown length, and bark thickness). Dead biomass consumption is simulated using functions of fire intensity and fuel moisture that are fuel-class specific.

Fire effects extend beyond the direct impact on carbon and nutrient pools to more indirect and complex effects on tree versus grass competition. Fire tends to tip the competitive balance toward grasses in the model because much, or all, of the grass biomass consumed regrows in the year after a fire event. Woody biomass consumed or killed is more gradually replaced. A greater competitive advantage over trees promotes greater grass biomass. This, in turn, produces higher fine fuel loadings and changes in the fuel bed structure that promote greater rates of spread and thus more extensive fire. In contrast to the simulated rate of spread, which is largely dependent

on fine fuel properties, fire-line intensity is more dependent on the properties of the total fuel load. Thus, an increase in tree biomass, which contributes more to the heavy coarse fuels, promotes more intense fire and more biomass consumption and mortality. This, in turn, acts as another negative effect on tree biomass. However, increases in tree biomass also reduce the productivity of grasses, which reduces both fine fuel and total fuel loadings, adding another layer of complexity to the fire-vegetation interactions in the model.

2.2 Climatic Data

The climate data used as input to the model in this study consisted of monthly time series for all the necessary variables (i.e., precipitation, minimum and maximum temperature, and vapor pressure) distributed on a 100 km^2 resolution data grid for the state of California. Spatially distributed monthly time-series data for historical (1895-1993) precipitation, temperature, and vapor pressure already existed at a 100 km^2 resolution. This dataset was developed from a subset of climate data generated by VEMAP (Kittel et al., 1997) and from observed California station data interpolated to the data grid by the PRISM model (Daly et al., 1994). Incremental climate scenarios were also developed; the attachment to this appendix describes the development of these incremental scenarios and the simulation results obtained.

To construct spatially distributed climate time-series datasets for the two potential future climatic periods (1994-2100) of our simulations, we used coarse-scale monthly output generated by two general circulation models (GCMs) — the Hadley Climate Center HadCM2 model and the National Center for Atmospheric Research (NCAR) parallel climate model (PCM). Both are state-of-the-art GCMs that include the influence of dynamic oceans and aerosol forcing on the atmosphere. Most GCM experiments predict a warmer and wetter future for California. That prediction is represented in this study by the HadCM2 scenario (Mitchell and Johns, 1997). The PCM scenario (Dai et al., 2001) predicts a generally warmer and drier California, and thus provided a useful contrast to the HadCM2 scenario for testing the model's sensitivity to climatic change. Both GCM models were run from the 1800s to 1995 using observed increases in greenhouse gas concentrations, and into the future using Intergovernmental Panel on Climate Change (IPCC) projections of a 1% increase per year (Kattenberg et al., 1996). Using a methodology that is the accepted norm for creating higher resolution climate scenarios for impact studies, we downscaled the two coarse-scale GCM scenarios to the 100 km^2 resolution. The steps in the development of the scenarios were

- For each climate variable, monthly averages were calculated for the 1961-1990 GCM-simulated climate for each coarse-scale GCM grid cell over California.

- At each GCM grid cell and for each future simulation month, "deltas" were calculated between the long-term average for each variable (from step 1) and the value for the

"target" month taken from the GCM-simulated time series (deltas were calculated as differences for temperature variables, and as ratios capped at 5 for precipitation and vapor pressure).

- The deltas for each variable were interpolated to a 100 km^2 resolution data grid using a quintic polynomial interpolation procedure.

- The interpolated deltas were applied back to a 100 km^2 resolution grid of means observed from 1961 to 1990 to create a high-resolution, gridded time series of possible future weather based on the coarse-grid GCM output.

Distinctly different trends of mean annual temperature and total annual precipitation emerge under the two future climate scenarios (Figure 2). Both scenarios show an increase in annual temperature relative to the mean for the historical base period (labeled "HIST" on the figure), but the increase is significantly greater for the HadCM2 scenario. The two scenarios are even more distinct in terms of projected trends in precipitation. The HadCM2 scenario is wetter and the PCM scenario is drier than the historical average for most years, but the contrast between the two is especially pronounced in the last few decades of the future period.

A change in the seasonal trend of temperature and precipitation may have as much impact on ecosystem properties as changes in annual trends. Average monthly values for temperature and precipitation over the 30 year historical base period (Figure 3) show the characteristic trends for a Mediterranean climate with cool wet winters and hot dry summers. For both scenarios, monthly temperature and precipitation averaged over the future 30 year period retain these seasonal trends. Every month is warmer under both scenarios, but winter and summer months in the HadCM2 scenario show the greatest increase in temperature. The most striking feature of future monthly precipitation under the wetter HadCM2 scenario are the relatively large increases projected for the winter months in contrast to the much smaller increases in the summer, which in effect amplifies the Mediterranean winter-wet and summer-dry cycle. The PCM scenario shows less of a departure from the historical trend, with monthly changes consisting mostly of consistently small decreases in precipitation.

The future climate scenarios are also distinguished by differences in the spatial distribution of projected changes in annual temperature and precipitation (Figure 4). Averaged over the 30 year period in the future (2070-2099), both temperature scenarios show a similar longitudinal gradient that extends from relatively large temperature increases east of the major mountain axes to relatively small changes to the west. In the HadCM2 scenario, this gradient is interrupted in southern California where projected changes in temperature are uniformly small. The distribution of change in average annual precipitation also distinguishes the two scenarios. For the HadCM2 scenario, precipitation increases across the entire state, in contrast to the wholesale decrease for the PCM scenario. The distribution for the HadCM2 scenario shows a nearly latitudinal

A.

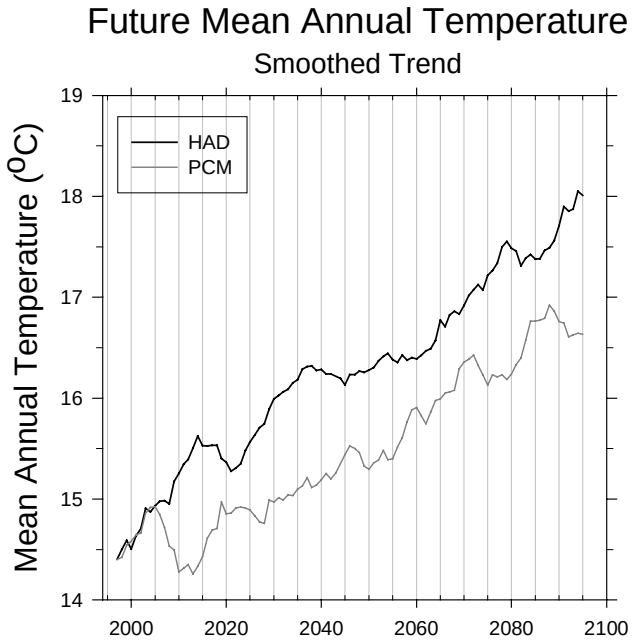

B.

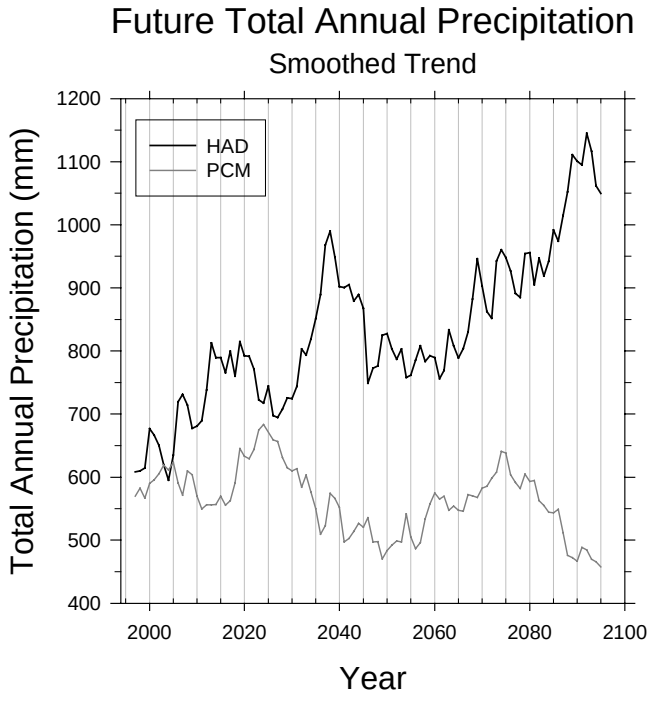

Figure 2. Future trends in (a) mean annual temperature and (b) total annual precipitation under the HadCM2 and PCM future climate scenarios. Annual values are averages across all grid cells. Trends were smoothed for display using a 10 year running average.

A.

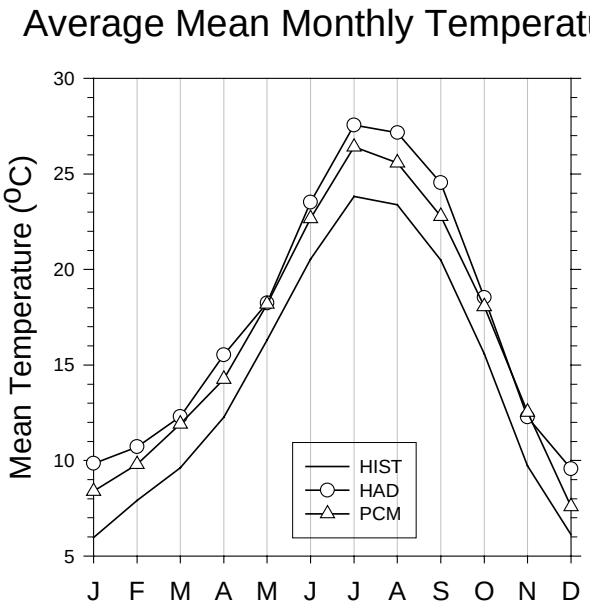

B.

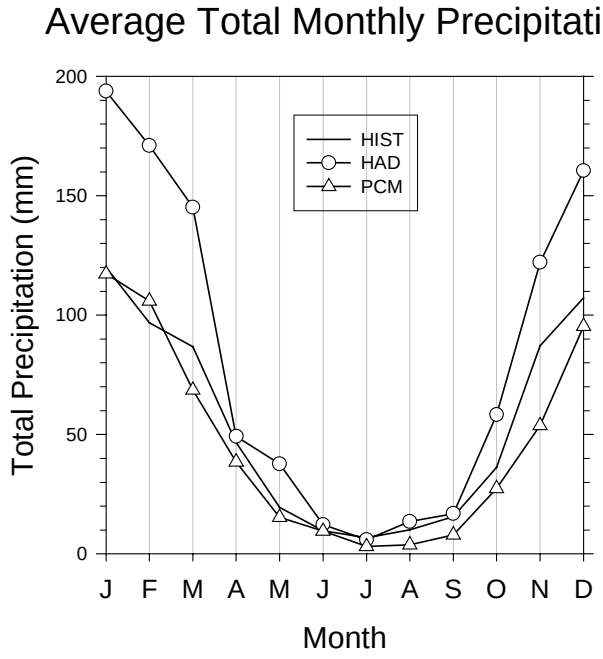

Figure 3. Seasonal trends in (a) mean monthly temperature and (b) total monthly precipitation trends for the historical period (1961-1990) and the future period (2070-2099) of the HadCM2 and PCM future climate scenarios. Monthly values are averages for the time period and across all grid cells.

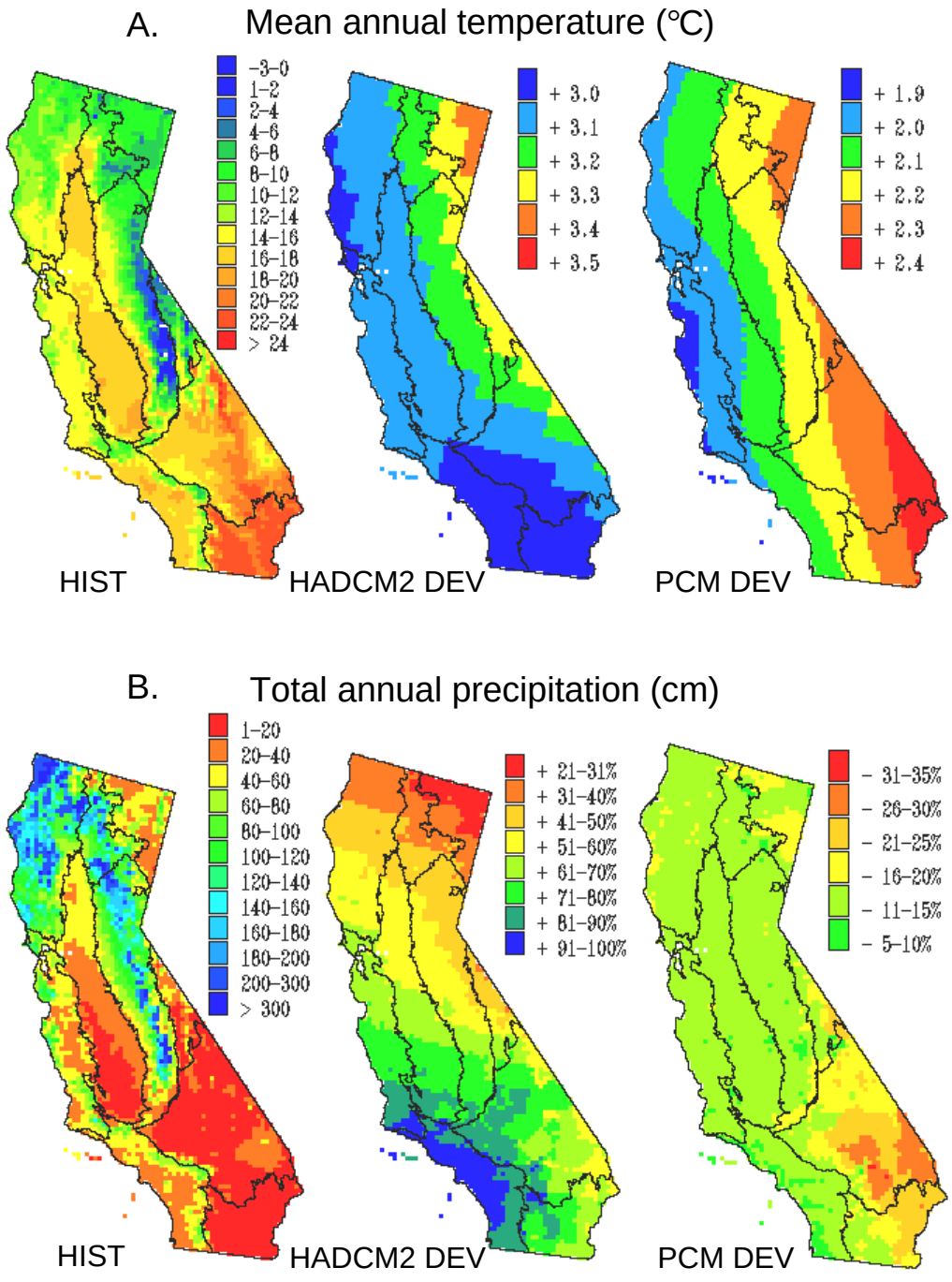

Figure 4. The spatial distribution of (a) mean annual temperature and (b) mean total annual precipitation for the historical period (1961-1990) and for changes in same for the future period (2070-2099) under the HadCM2 and PCM climate scenarios. Future changes are relative to the historical period.

gradient of increased precipitation, which makes southern California (and especially the coastal sector) the region with the greatest percentage increase. There is no statewide spatial gradient in precipitation decline for the PCM scenario. Both the smallest and largest changes occur in southern California. The smallest percentage decreases in annual precipitation tend to occur in the coastal sector; the relatively large percentage declines occur mainly in the desert sector.

3. Results and Discussion

3.1 Simulation Results for the Historical Climate

3.1.1 Vegetation classes

Of the 22 possible vegetation types predicted by the biogeography module, 12 occurred in the simulations for California. These types were aggregated into seven vegetation classes to simplify the visualization of results. The aggregation scheme and lists of typical regional examples in each vegetation class (Table 1) indicate the range of each class in terms of physiognomy and species dominance.

Table 1. MC1 vegetation type aggregation scheme and regional examples of the vegetation classes

MC1 vegetation class	MC1 vegetation type	Regional examples
Alpine/subalpine forest	Tundra	Alpine meadows
	Boreal forest	Lodgepole pine forest
		Whitebark pine forest
Evergreen conifer forest	Maritime temperate conifer forest	Coastal redwood forest
	Continental temperate coniferous forest	Coastal closed-cone pine forest
		Mixed conifer forest
		Ponderosa pine forest
Mixed evergreen forest	Warm temperate/subtropical mixed forest	Douglas fir/tan oak forest
		Tan oak/madrone/oak forest
		Ponderosa pine/black oak forest
Mixed evergreen woodland	Temperate mixed xeromorphic woodland	Blue oak woodland
	Temperate conifer xeromorphic woodland	Canyon live oak woodland
		Northern juniper woodland
Grassland	C3 grassland	Valley grassland
	C4 grassland	Southern coastal grassland
		Desert grassland
Shrubland	Mediterranean shrubland	Chamise chaparral
	Temperate arid shrubland	Southern coastal scrub
		Sagebrush steppe
Desert	Subtropical arid shrubland	Creosote brush scrub
		Saltbrush scrub
		Joshua tree woodland

The results of the vegetation class simulation for the historical period are shown in Figure 5a as the distribution of the most frequent vegetation type simulated for the 1961-1990 climate period. The simulated vegetation class distribution is difficult to validate against different maps of vegetation available for California. The MC1 biogeography module simulates the life form mixture and vegetation type that could potentially occur given climatic conditions and the simulated fire regime. Many of the available vegetation maps show that the distribution of vegetation types is highly modified by urbanization, agriculture, and forestry practices, including fire suppression. Others show the distribution of potential vegetation types, but comparisons to these involve difficulties associated with different criteria for classification and potential errors associated with crosswalking different classification schemes. The Küchler (1975) potential vegetation map of the United States was selected as a baseline for comparison against the vegetation class simulation for the historical period. A baseline vegetation map was created for California by aggregating the 28 vegetation types mapped by Küchler in California into the seven vegetation classes simulated by MC1 (Figure 5b).

The overall distribution of the vegetation classes simulated for the historical period (Figure 5a) was very similar to their distribution on the baseline vegetation map (Figure 5b). The percentage of coverage of the vegetation classes for the MC1 simulation also compared favorably to the baseline map (Figure 6). However, a few notable differences can be seen in terms of both distribution and coverage within the different bioregions. For example, MC1 predicted greater coverage of mixed evergreen forest, especially along the western slope of the Sierra Nevada where the baseline map shows evergreen conifer forest. In the central western region, MC1 predicts a mixture of evergreen conifer forest and mixed evergreen forest along the coast where the baseline map shows evergreen woodland and shrubland. Other somewhat smaller discrepancies occur in the southwestern region and at the southern end of the Sierra Nevada where the MC1 simulation shows more grassland than the baseline map, and in the eastern half of the Cascade Range region where MC1 predicted more shrubland.

Not all the instances where the simulated vegetation class distribution differs with the baseline distribution are necessarily errors in the simulation. For example, on the baseline map there is no mixed evergreen forest in the region between mixed evergreen woodland and evergreen conifer forest along the western slope of the Sierra Nevada. However, a Sierran mixed hardwood forest with a strong resemblance to the mixed evergreen forests of the coastal mountains has been described for this region (Holland and Keil, 1995). The simulated occurrence and distribution of evergreen conifer and mixed evergreen forest along the coastal sector of the central western region is also supported by descriptions of closed-cone coniferous forest and mixed hardwood forest (Holland and Keil, 1995; Sawyer et al., 1995; Vogel et al., 1995) for this region of California.

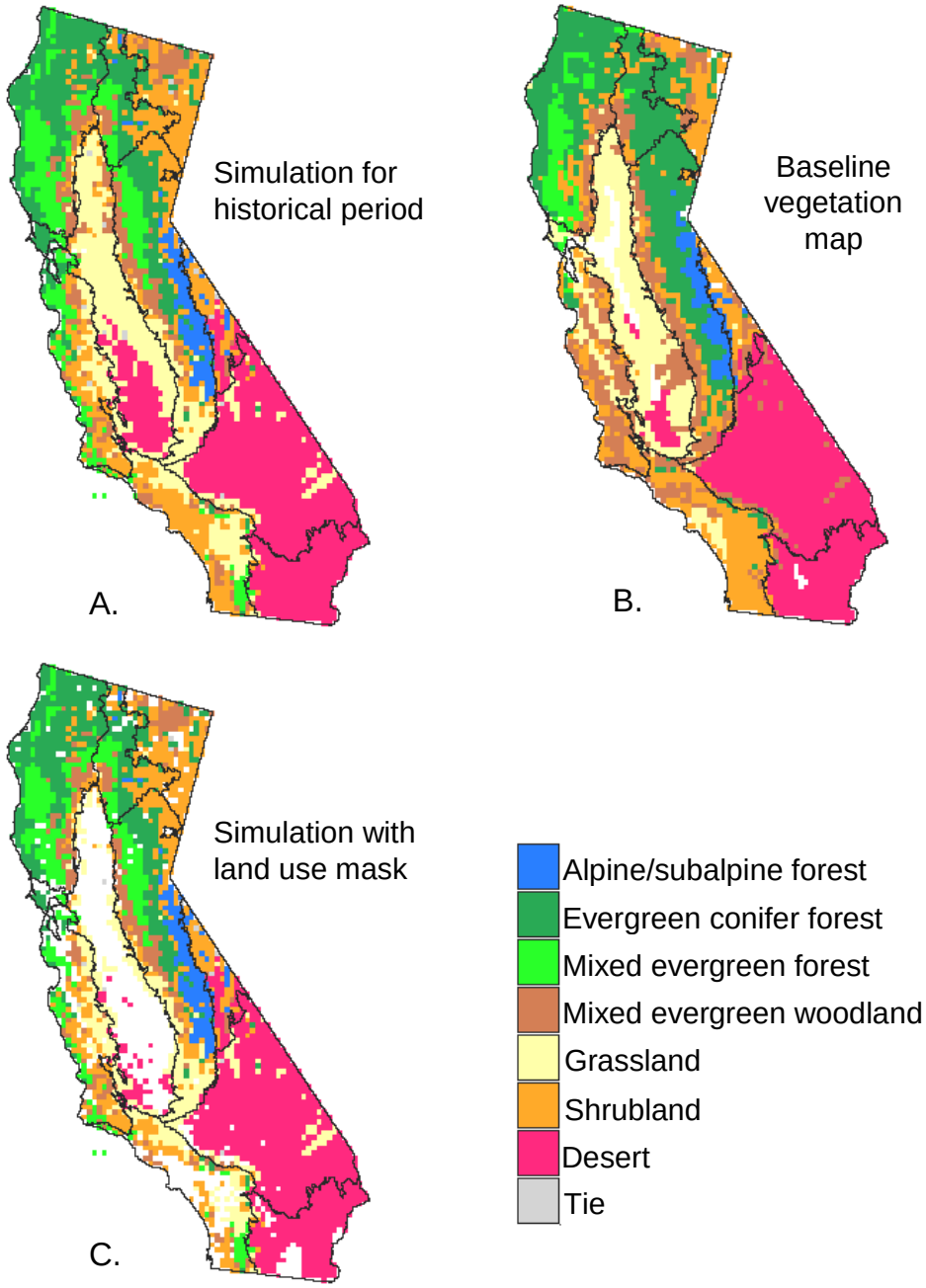

Figure 5. Maps of the (a) distribution of the simulated vegetation classes for the historical period (1961-1990), (b) baseline vegetation map, and (c) historical simulation with urban and agricultural areas masked out. The vegetation class mapped at each grid cell in (a) and (c) are the most frequent class simulated during the historical period. A "tie" is where two or more classes were equally frequent.

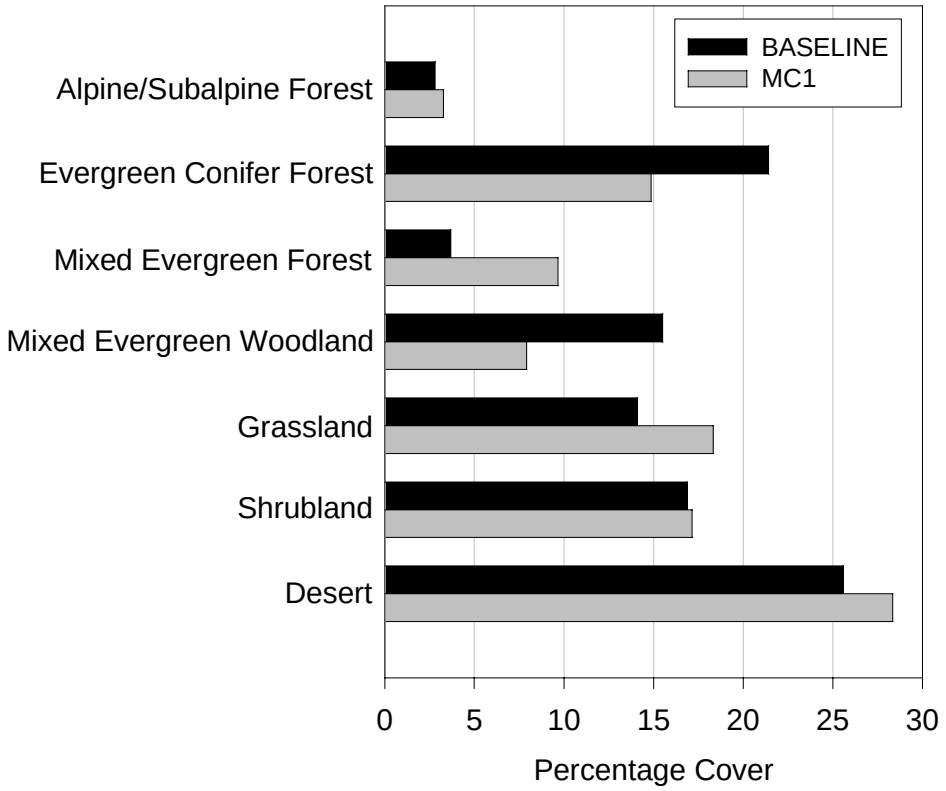

Figure 6. Percentage land cover of vegetation classes for the historical period (1961-1990) simulation compared to the baseline vegetation map

3.1.2 Carbon density

Average carbon density values for the simulated vegetation classes (Table 2) compared favorably to observed mean carbon density values derived for equivalent vegetation classes (Atjay et al., 1979; Houghton and Hackler, 2000). The distribution of simulated average total ecosystem carbon (Figure 7a) and average total vegetation carbon (Figure 7b) for the 30 year historical period also appears to be relatively accurate, with the highest carbon density in the most heavily forested regions of the state (i.e., the Northwest, Cascade Range, and Sierra Nevada regions), the lowest carbon density in the most arid regions (i.e., the Mojave and Sonoran deserts), and intermediate values throughout the rest of the state. This carbon density gradient is even more distinct in the distribution of live tree carbon (Figure 8a) where the highest values clearly define the forested portion of the state. The distribution of grass carbon density (Figure 8b) is negatively

Table 2. Observed versus simulated values for total ecosystem carbon in major vegetation classes[a]

	Total carbon (kg/m^2)	
Vegetation class	**Observed**	**Simulated**
Evergreen conifer forest	25	21
Woodland	18	14
Shrubland	12	14
Grassland	9	13
Desert	8	9

a. Simulated values are mean annual values for the historical period (1961-1990) average across the state. Observed values estimates for the United States were reported by Houghton and Hackler (2000) and Atay et al. (1979).

related to the distribution of woody carbon density, and the highest grass values are simulated in regions of the state (e.g., the Central Valley and surrounding foothills, southern coast, and intermountain basin) where grassland likely was a dominant element of presettlement vegetation (Barbour and Major, 1988; Holland and Keil, 1995).

3.1.3 Fire regime

The MC1 fire module simulates fire severity under conditions of potential natural vegetation and no fire suppression, so validating the historical simulation of fire involves some of the same difficulties described for the vegetation class simulation. The simulated distribution of fire rotation period (i.e., the expected time to burn an area the size of the grid cell; Heinselman, 1973), which was calculated for the 100 years of historical climate (Figure 9a), showed that, for more than 90% of the state, the rotation period was about 6 to 20 years. Taking the fire rotation period as an estimate of point fire frequency (Lertzman et al., 1998), this result compares favorably with observed point-based frequencies of 5 to 10 years in woodlands and grasslands and 4 to 20 years in mixed and conifer forests of California (Skinner and Chang, 1996). Considerably longer mean fire rotation periods of 20 to 100 years were simulated for coastal forests and shrublands where fire activity is constrained by relatively high humidity and fuel moisture, and in the most arid portions of the state where fire activity is constrained by relatively low fuel loads.

The thresholds of drought and fine fuel flammability that trigger fire events in the MC1 fire module are set to constrain events to those of relatively high intensity and severity. The distribution of fire-line intensity (Figure 9b) averaged over all fire events in the 100 year historical simulation is consistent with the distribution of vegetation classes and their characteristic fire behaviors under severe burning conditions. Rothermel (1983) provides a

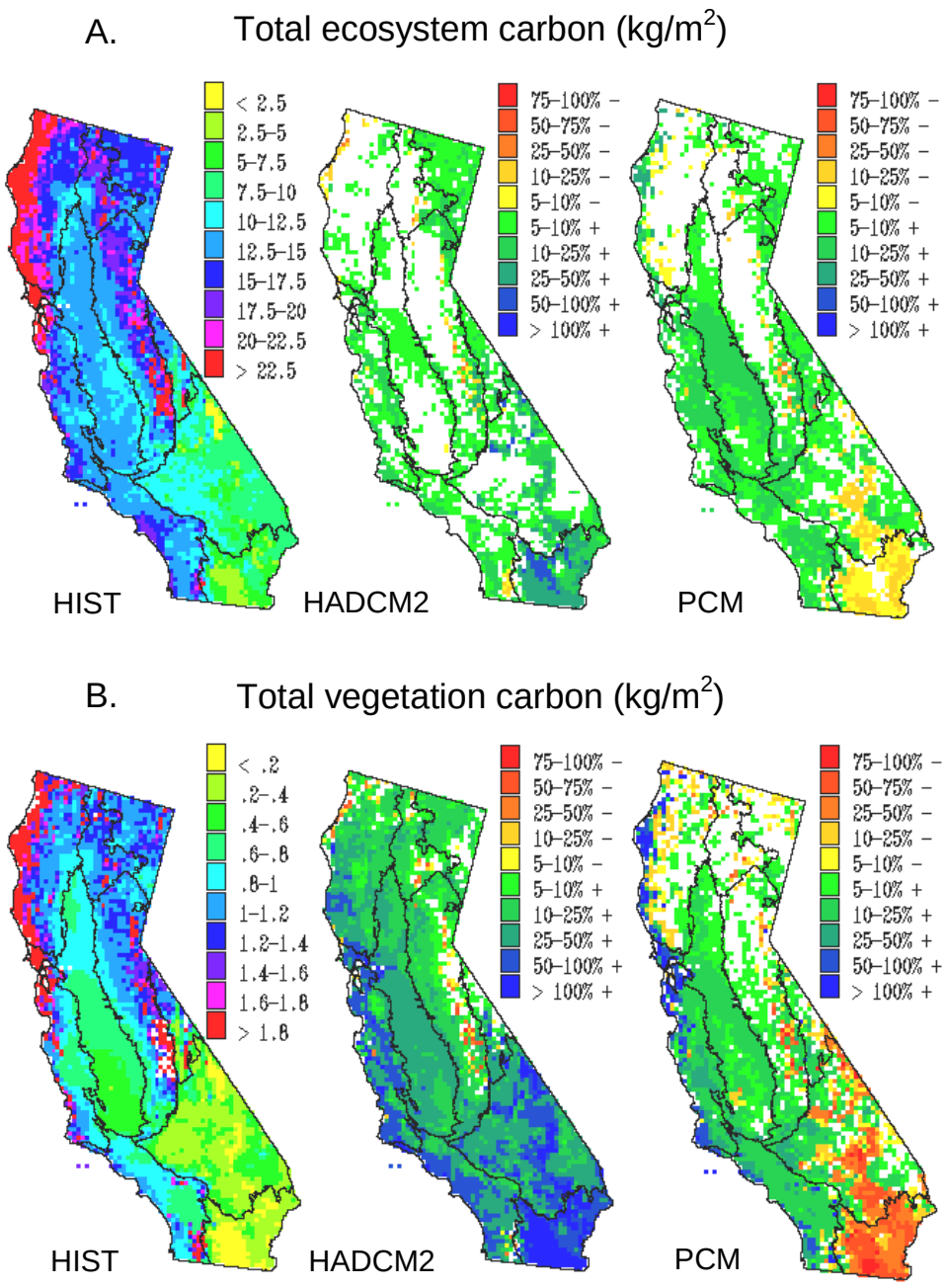

Figure 7. The distribution of (a) average total ecosystem carbon and (b) average annual total vegetation carbon for the historical period (1961-1990) simulation and for simulated changes in same for the future period (2070-2099) of the HadCM2 and PCM climate scenarios. Future changes are relative to the historical period.

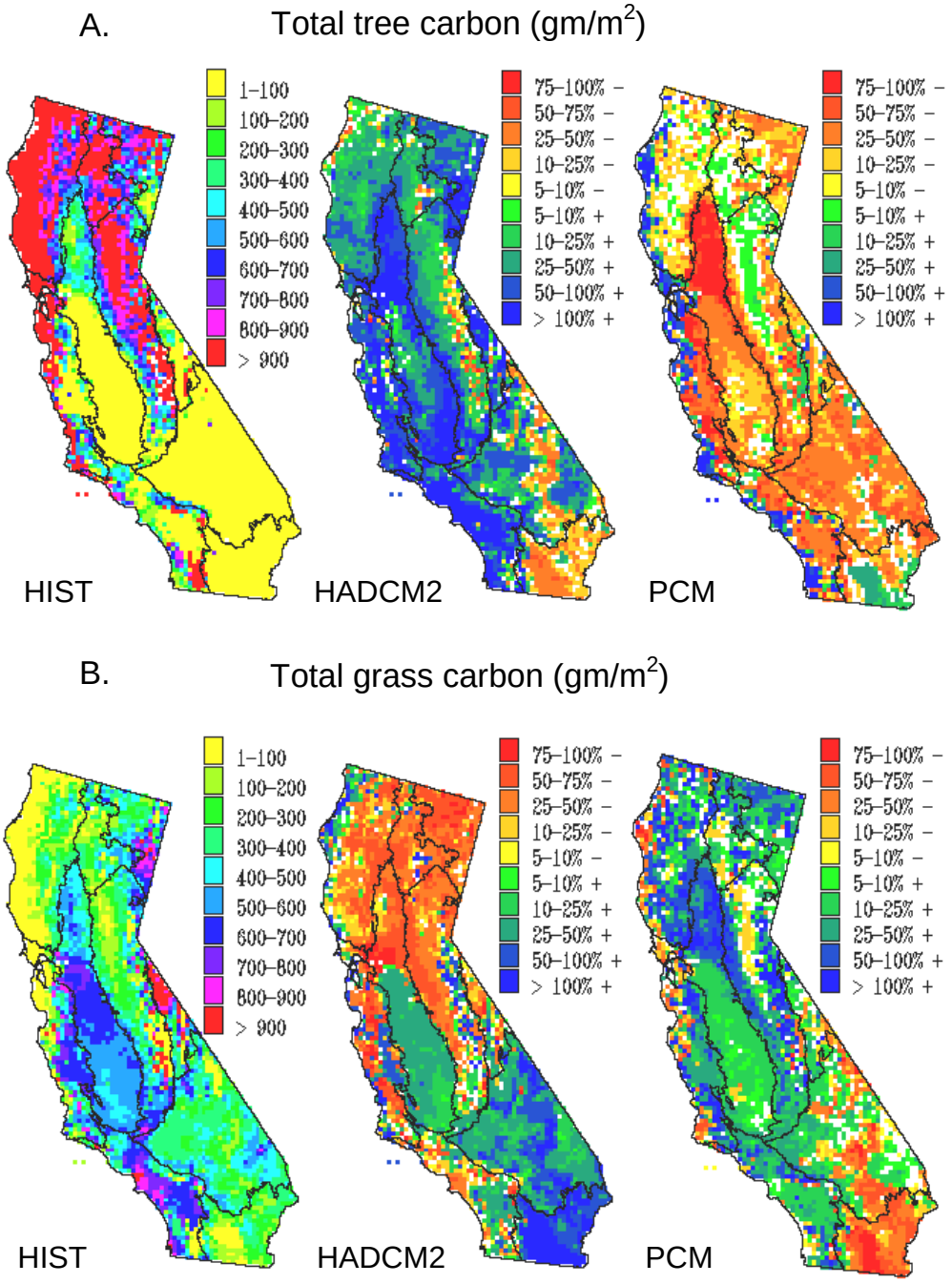

Figure 8. The distribution of (a) average tree carbon and (b) average grass carbon for the historical period (1961-1990) simulation and for simulated changes in same for the future period (2070-2099) of the HadCM2 and PCM climate scenarios. Future changes are relative to the historical period.

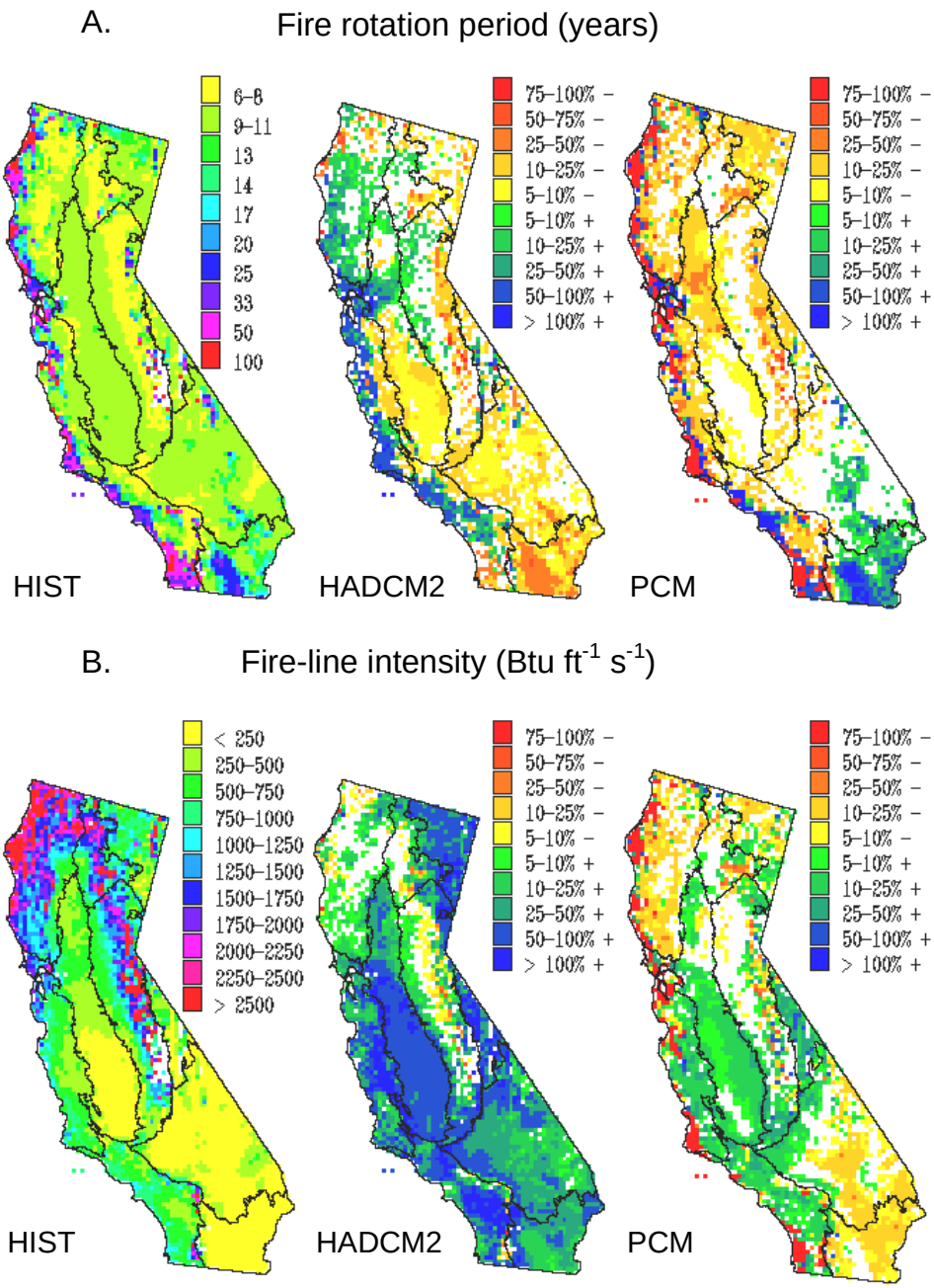

Figure 9. The distribution of the (a) fire rotation period and (b) average fire-line intensity per event for the historical period (1895-1994) simulation and for simulated changes in same for the future period (2000-2099) of the HadCM2 and PCM climate scenarios. Future changes are relative to the historical period.

classification of fire-line intensities characteristic of surface fire (<500 Btu/ft/s), mixed surface and passive crown fire (500-1,000 Btu/ft/s), and active crown fire (>1,000 Btu/ft/s). By this measure, the historical intensities simulated by MC1 are primarily in the range of crown fire in the forest classes, the mixed fire regime in the woodlands and shrubland classes, and surface fire in the grasslands and desert classes.

Martin and Sapsis (1995) estimated that fire burned 5.5% to 13.0% of California annually under presettlement conditions. The range of percentage of area burned simulated by MC1 during the 100 years of the historical simulation (6.3%-15.5%; Figure 10) was remarkably similar to this independent estimate. The simulated trend of percentage of area burned showed a significant and fairly strong relationship (Spearman rank correlation = -0.70, $p < 0.001$) with the historical trend of the Palmer's Z drought index (Figure 10) for California. Statewide values of the index for the period of record were calculated by averaging over values for all five climatic divisions in California (Karl, 1986). Several of the most severe fire years simulated by the model were coincident with some of the most severe drought years (e.g., 1910, 1924, 1928, 1959, and 1966), and several of the least severe fire years correspond to some of the wettest years (e.g., 1906, 1912, 1941, 1958, and 1983). Another pattern evident in the relationship between simulated fire and the drought index was the occurrence of a wet episode 1 or 2 years preceding a dry and severe fire year (e.g., 1906 and 1908, 1958 and 1959, 1982 and 1983, and 1984). Several of the most severe fire years (e.g., 1908, 1959, and 1984) were preceded by one or more relatively wet years in which a buildup of fuels was simulated by the model. A similar pattern of large fire years promoted by sequences of wet seasons followed by average or drier than average seasons has been identified in the southwestern United States (Swetnam and Betancourt, 1998).

In an attempt to validate the simulated trend of area burned during the historical period, the simulation results were compared to the observed trend on U.S. national forest lands within the Sierra Nevada bioregion during the 1908-1993 period (McKelvey and Busse, 1996). The simulated mean annual area burned for this region during the historical period (87 kha/yr) was significantly greater than the observed mean (17 kha/yr). It is likely that fire suppression and ignition constraints have reduced the observed mean annual area burned to some unknown level below the potential value estimated by the model (McKelvey and Busse, 1996, Husari and McKelvey, 1996). The observed and simulated trends (Figure 11) showed a significant but only moderately strong correlation (Spearman rank correlation coefficient = 0.52, $p < 0.001$). The observed data does validate the occurrence of several severe fire years simulated by the model (e.g., 1910, 1917, 1924, 1928, 1939, 1959, and 1987).

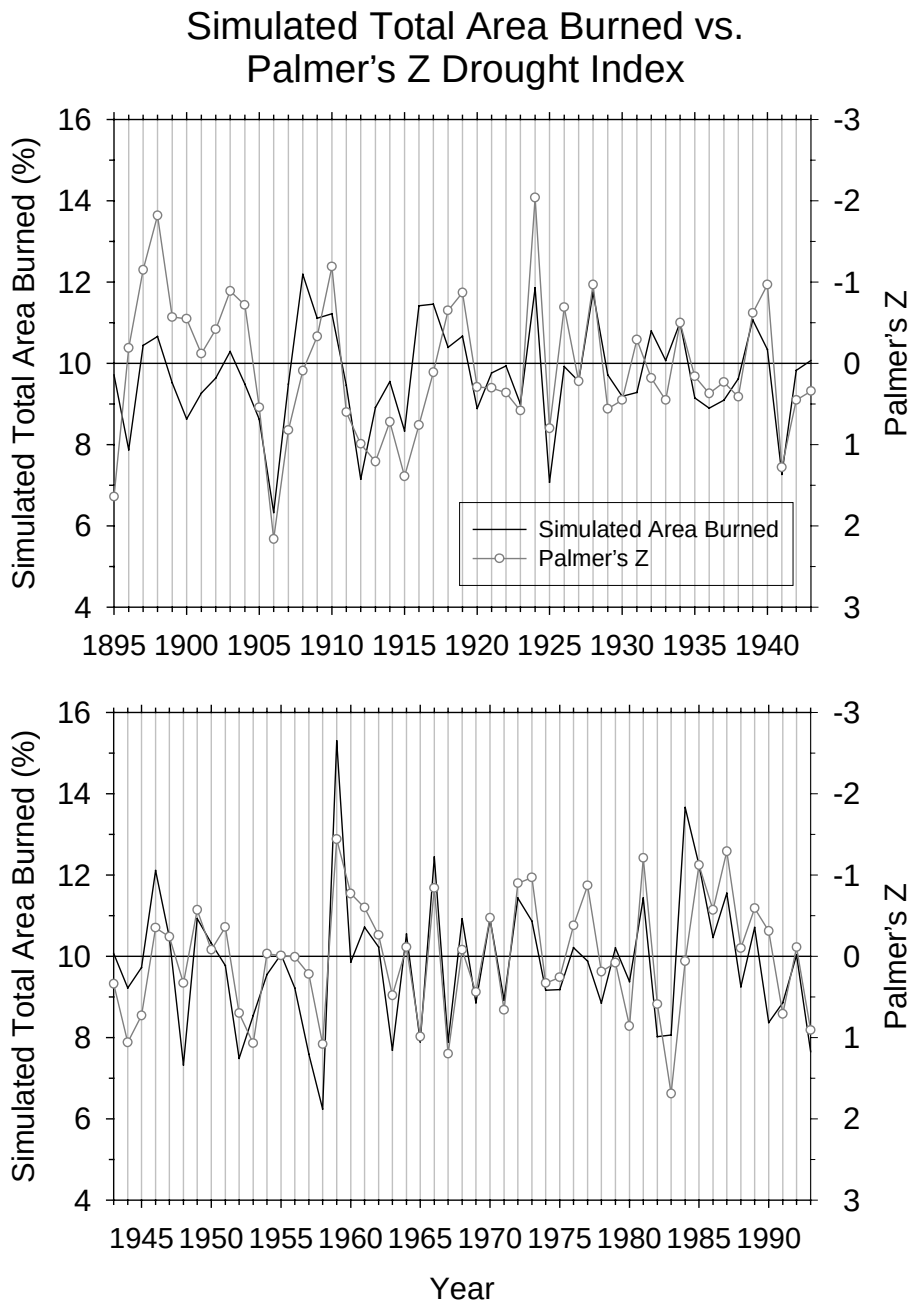

Figure 10. Trend in average summer month (June-August) moisture anomaly (Palmer Z) for the historical period (1895-1993) compared to the simulated trend in annual percentage of the total land area of California burned. Statewide values of Z for were calculated by averaging over values for all five climatic divisions in California (Karl, 1986).

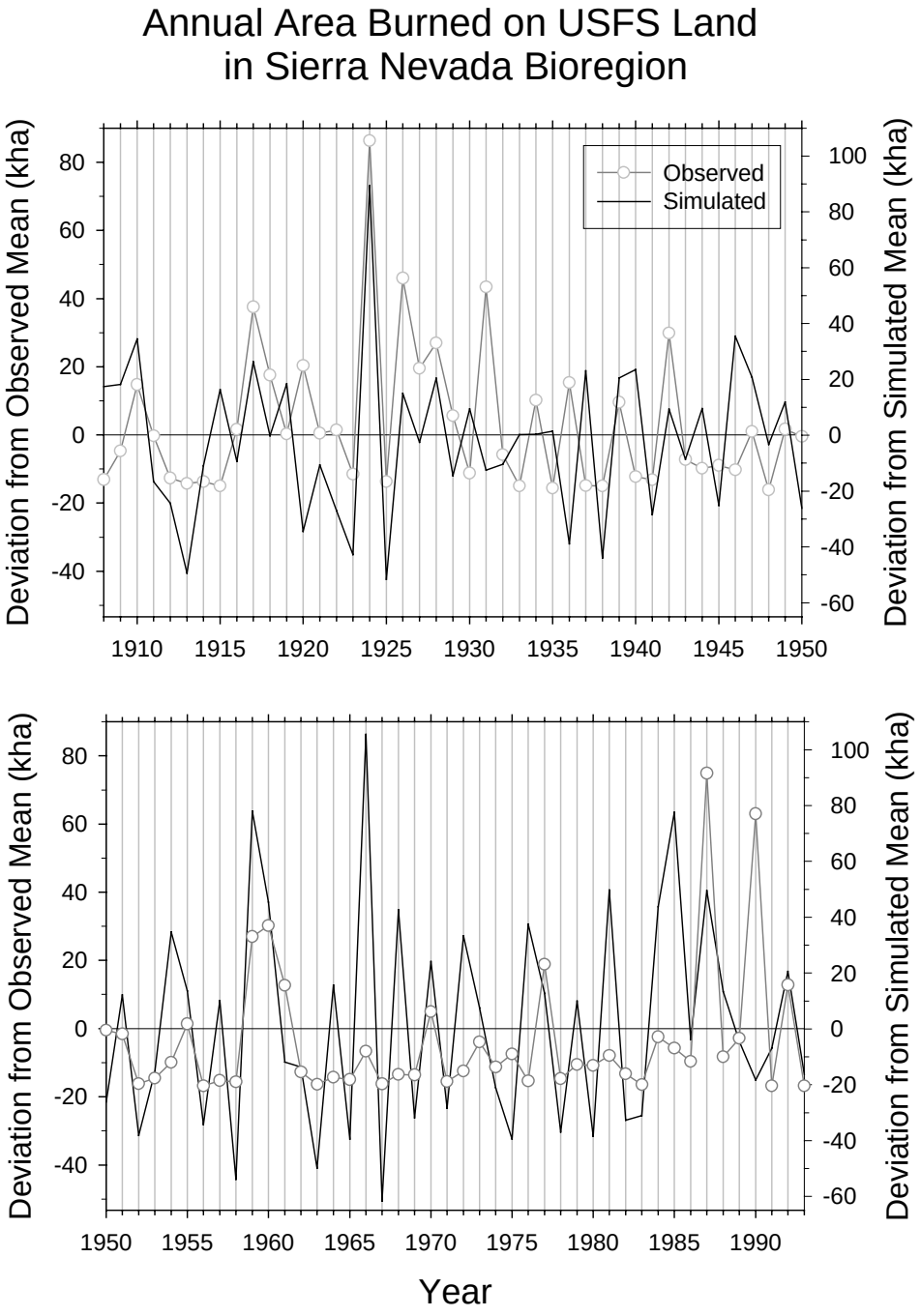

Figure 11. Simulated versus observed trends in deviations from the mean of annual area burned on U.S. Forest Service (USFS) land in California for the period 1908-1993. Simulated and observed means were 106 and 17 kha burned/year, respectively.

3.2 Simulations for the Future Climate Scenarios

3.2.1 Vegetation classes

The response of vegetation class distribution under the two future climate scenarios was determined by comparing the distribution of the most frequent vegetation type simulated for the 30 year historical period (Figure 12a) against the same for the last 30 years (2071-2099) of the future scenarios (Figure 12b,c). The retreat, advance, and stasis of each vegetation type were also mapped for each climate scenario (Figures 13 and 14). Retreat means that a vegetation class was present in the historical simulation but absent in the future simulation. Advance means that a vegetation type was absent in the historical simulation but present in the future simulation. Stasis means that the vegetation type occurred in both the historical and future simulations.

The simulated response of the vegetation classes in terms of changes in percentage of coverage (Figure 15) was surprisingly similar under the two future climates. There was agreement on the direction of change (i.e., decrease or increase in coverage) for all but the evergreen conifer forest class, and the amounts of change were comparable for a few of the vegetation classes. However, these similarities in the response of class coverage were often the net result of very different responses to each scenario in terms of the spatial distribution of vegetation classes.

3.2.1.1 HadCM2 scenario

A prominent feature of the response of the vegetation class distribution under the HadCM2 scenario (Figure 12b) was the advancement of forest classes into the Modoc Plateau, into the northern end of the Great Central Valley, toward higher elevations in the Sierra Nevada, and inland along the coast. Increases in both temperature and moisture under this scenario favored expansion of forest, and they were especially favorable for mixed evergreen forest (Figure 13b). The relatively high degree of warming under the HadCM2 scenario promoted a widespread change in the simulated life form composition from needleleaf dominance to mixed needleleaf-broadleaf in the northern half of the state. Consequently, mixed evergreen forest replaced evergreen conifer forest (Figure 13a) throughout much of the latter's simulated historical range. Two examples of this transition in terms of species dominance within the different bioregions might include the replacement of Douglas fir-white fir forest by Douglas fir-tan oak forest in the northwest bioregion, and the replacement of white fir-ponderosa pine forest by ponderosa pine-black oak forest in the Sierra Nevada. Greater moisture availability under the HadCM2 scenario also promoted the advancement of mixed evergreen forest (Figure 13b) into mixed evergreen woodland (Figure 13c), shrubland (Figure 13d), and grassland (Figure 13e). Movement into the northern end of the Great Central Valley could represent the replacement of blue oak woodlands, chaparral, and perennial grassland by tan oak-madrone-canyon live oak forest with scattered Douglas fir and ponderosa pine. In the central western and southwestern bioregions, mixed

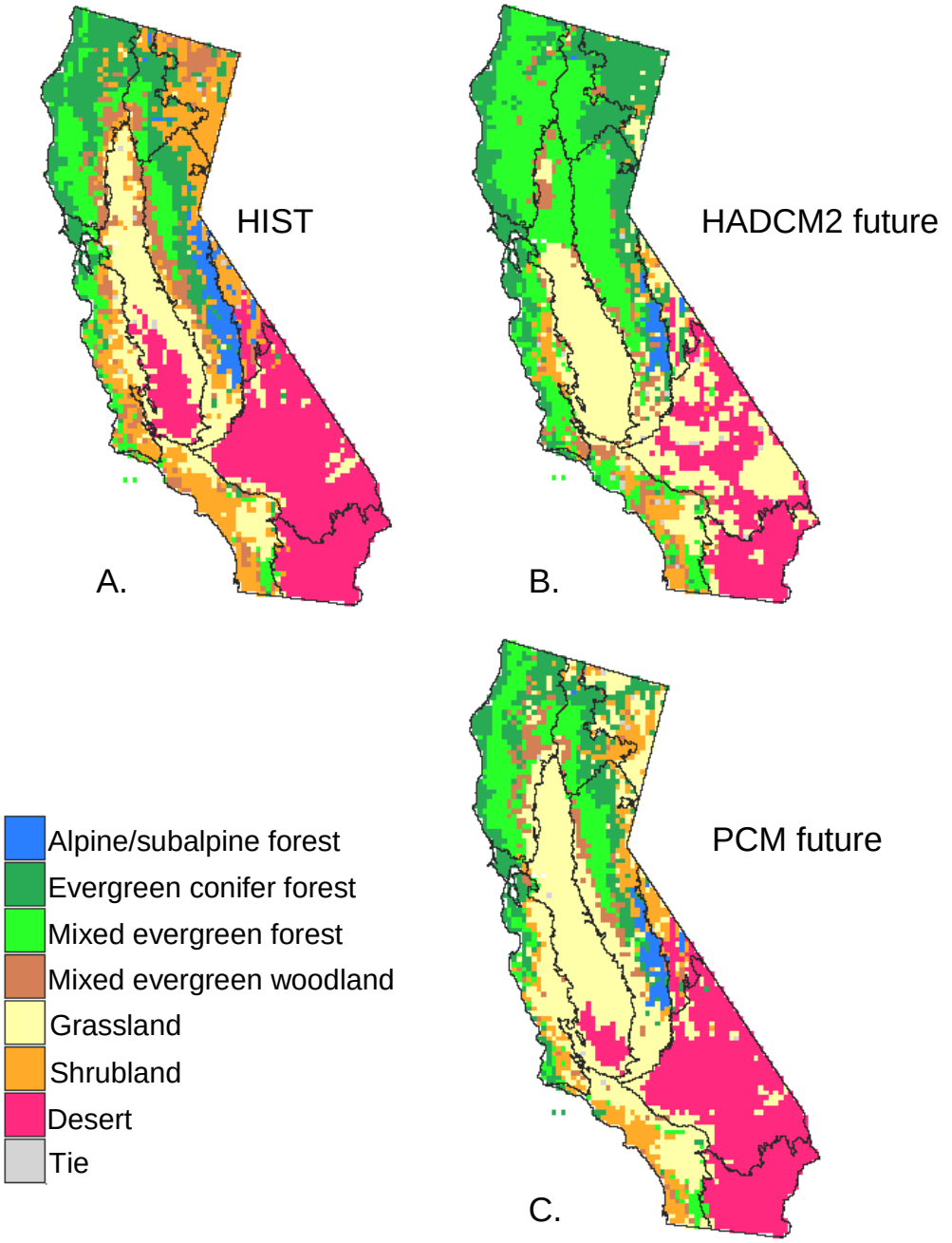

Figure 12. Distribution of the vegetation classes (a) simulated for the historical period (1961-1990) and (b,c) the future period (2070-2099) of the HadCM2 and PCM climate scenarios. The vegetation class mapped at each grid cell in is the most frequent class simulated during the time period. A "tie" is where two or more classes were equally frequent.

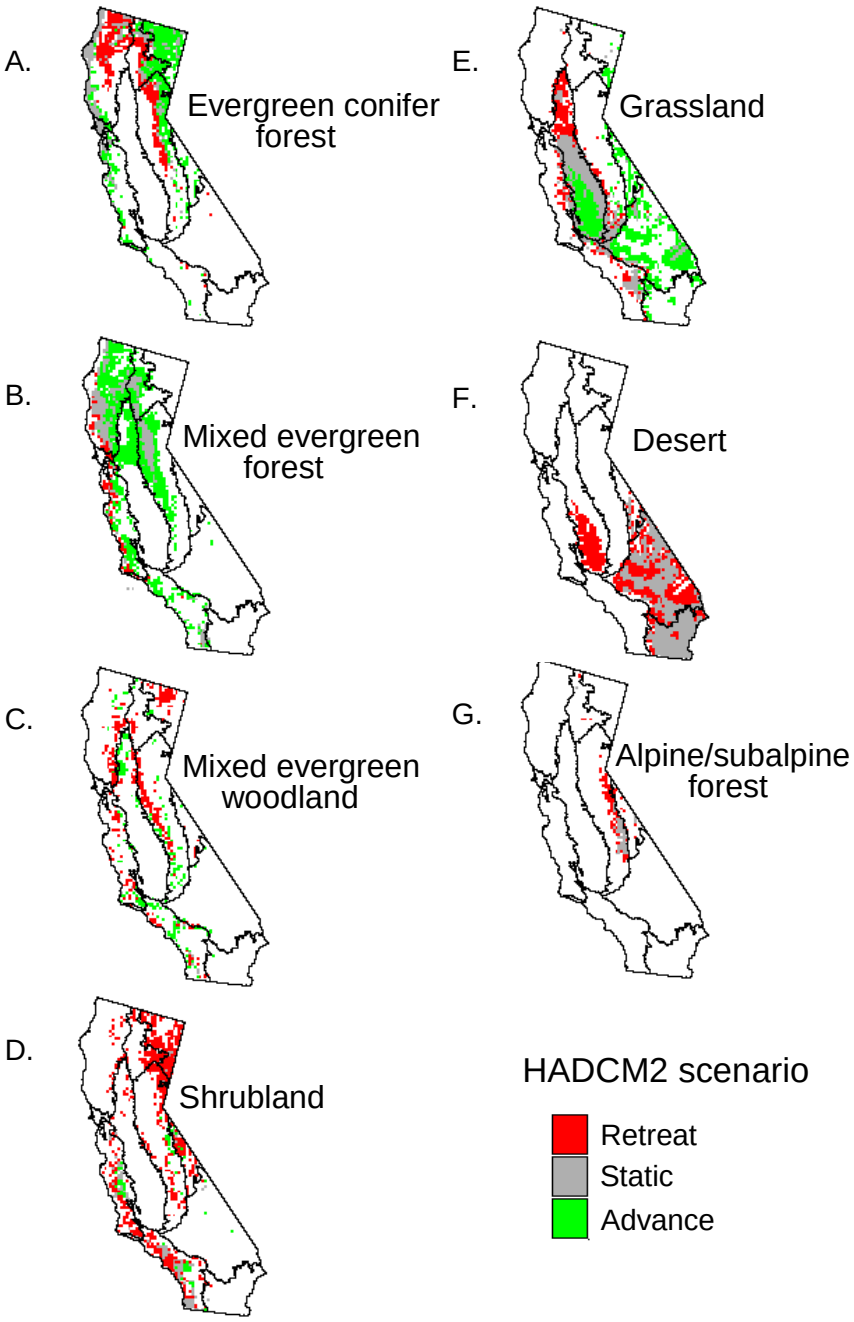

Figure 13. Simulated redistribution of the seven vegetation class (a-g) under the HadCM2 scenario. Changes are for the future period (2070-2099) relative to the historical period (1961-1990).

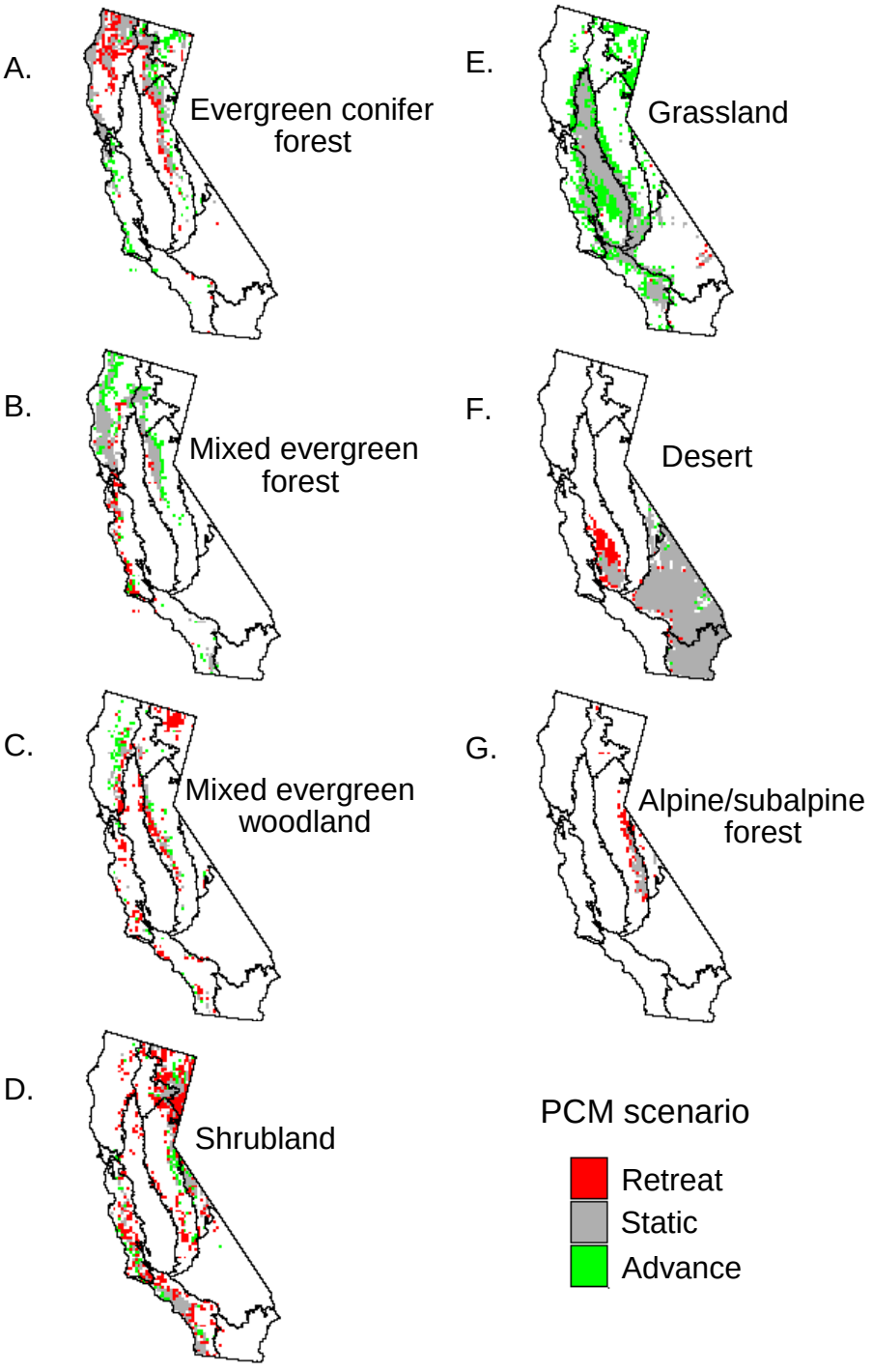

Figure 14. Simulated redistribution of the seven vegetation class (a-g) under the PCM scenario

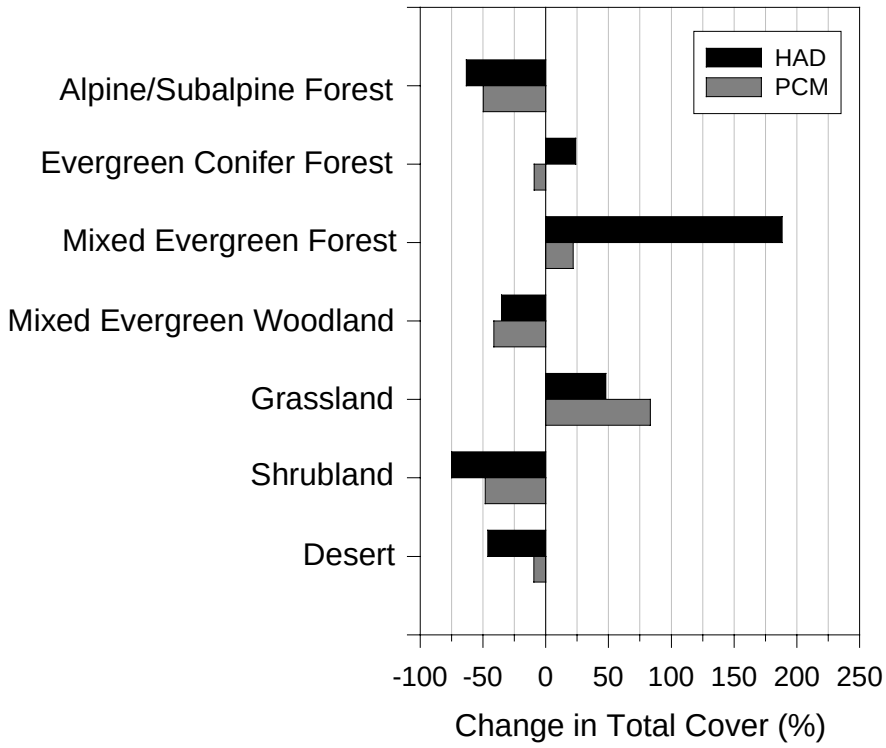

Figure 15. Percent changes in the total cover of the vegetation classes under the HadCM2 and PCM scenarios

evergreen forests of coast live oak-madrone or canyon live oak-Coulter pine might replace chaparral and live oak woodlands.

Evergreen conifer forest (Figure 13a) showed a net increase in percentage of coverage under the HadCM2 scenario despite the loss of much of its simulated historical range to mixed evergreen forest (Figure 13b). The main region of evergreen conifer advancement was in the cold desert region of the Modoc Plateau and east of the Sierra Nevada Range. Here higher moisture availability promoted the advancement of evergreen conifer forest into mixed evergreen woodland (Figure 13c) and shrubland (Figure 13d). On the Modoc Plateau, this transition would likely be characterized by replacement of northern juniper woodland and Great Basin sagebrush scrub by ponderosa pine-Jeffrey pine forest.

Maritime evergreen conifer forest, one of the MC1 vegetation types comprising the evergreen conifer vegetation class, is distinguished in the rule base by very high tree leaf carbon density and a low index of continentality (i.e., difference between highest mean monthly temperature and lowest mean monthly temperature) simulated for the relatively moist and equable climate along

the northern and central coast of California. In the historical simulation, these criteria effectively distinguished the conifer-dominated forests (e.g., redwood and closed-cone pine forests) along the north–central coast where effective moisture is high and temperatures are most equable. Advancement of this forest type under the wetter and warmer HadCM2 scenario (Figure 13a) would likely represent movement of redwood forest inland into the Douglas-fir-tan oak forest in the northwest bioregion, and expansion of redwood and closed-cone pines from remnant, fragmented groves into surrounding canyon live oak-madrone forests in the central western region.

Evergreen conifer forest (Figure 13a) also advanced into the high-elevation subalpine/alpine forest (Figure 13g) in the Cascade Range and Sierra Nevada regions under the HadCM2 scenario. Here the model responded to an increase in the length of the growing season past a threshold in the biogeographic rule base. Advancement of red fir or lodgepole pine forest into subalpine parks and meadow would be a likely example of this transition.

In addition to widespread advancement of forest, another prominent feature of the response of vegetation distribution under the HadCM2 scenario was the advancement of grassland (Figure 13e), particularly in the southern end of the Great Central Valley and in the uplands of the Mojave Desert where grassland replaces desert (Figure 13f). Here the response to increased precipitation was an increase in both tree and grass biomass (Figure 8a,b), and more fine fuels supported more fire (Figure 9a) that favored grasses. In the Mojave Desert, this transition could represent an increase in the extent of the desert grasslands interspersed with Joshua tree desert woodland and creosote bush scrub.

3.2.1.2 Parallel climate model scenario

The most prominent feature of the vegetation class response to the drier PCM scenario (Figure 12c) was the advancement of grassland (Figure 14e) into the simulated historical range of mixed evergreen woodland (Figure 14c) and shrubland (Figure 14d). This transition was prompted by a decline in the competitiveness of woody life forms relative to grasses as a response to a decline in effective moisture, and an increase in fire, which further constrained woody life form production. The advancement of grassland (Figure 14e) occurred primarily on the Modoc Plateau, in the foothills surrounding the Great Central Valley, and in the interior of the central western region. On the Modoc Plateau, a likely example of this transition would be an increase in the extent of the grassland that is interspersed within the northern juniper woodland and sagebrush scrub communities. A similar transition is already occurring under present-day conditions in the sagebrush scrub communities of the intermountain west. Here drought, increasing cheatgrass abundance, and fire are interacting to significantly reduce the woody scrub component (D'Antonio and Vistousek, 1992). In the foothills of the Great Central Valley and the

central western bioregions, the model simulation could indicate the loss of various oak woodland and chaparral communities to non-native grassland advancement.

Mixed evergreen woodland (Figure 14c) and shrubland (Figure 14d) show too little advancement to compensate for the retreat from grassland (Figure 14e) under the PCM scenario. Consequently, a net decline is seen in the coverage of mixed evergreen woodland and shrubland (Figure 15), along with a narrowing of the simulated ecotones between forest and grassland (Figure 12a and c). One local exception to this trend is in the eastern half of the northwest region, where there was some mixed evergreen woodland (Figure 14c) advancement into forest. In this bioregion, northern oak woodland advancing into Douglas fir-tan oak and Douglas fir-white fir forests would be likely example of this transition. An exception to the general decline in shrubland (Figure 14d) was in the Sierra Nevada region where shrubland advanced into alpine/subalpine forest (Figure 14g). Here a regional example of the model's response to a lengthened growing season could be an increase in whitebark pine krummholtz within alpine meadow communities.

In contrast to the simulation for the HadCM2 scenario, the distribution of mixed evergreen forest (Figure 14b) and evergreen conifer forest (Figure 14a) remained relatively static under the PCM scenario. Mixed evergreen forest showed a relatively small gain in coverage (Figure 15) with limited advancement into evergreen conifer forest in the northwest and Sierra Nevada bioregions. This transition was prompted by a temperature-driven shift in life form composition similar to that seen under the HadCM2 scenario, but the response was more constrained under the cooler PCM scenario. There was a net loss in the statewide coverage of evergreen conifer forest (Figure 15), but the class showed some advancement at high elevations in the Sierra Nevada and on the Modoc Plateau, and along the coast in the central western region (Figure 14a). In these relatively cool regions of the state, tree productivity increased as a response to increases in temperature and relatively small declines in precipitation.

3.2.2 Carbon density and fire regime

3.2.2.1 HadCM2 scenario

Underlying the advance of the forest classes under the HadCM2 scenario was an even more widespread increase in tree carbon density (Figure 8a). Tree biomass increased as a response to increased total annual precipitation and the amplification of the winter wet and summer dry seasonal cycle, both of which favored increased tree growth. The amount and distribution of tree biomass was strongly related to total annual precipitation. For example, the 500 mm isoline for the total annual precipitation was a consistently accurate predictor of tree leaf biomass at the threshold level between the woody vegetation classes and grassland in the simulations for the historical and future climate periods. And in the HadCM2 scenario, precipitation falling in

months outside the growing season was an even greater proportion of the total than had been seen historically (Figure 3b), and this favored trees over grasses in the simulated competition for water. Precipitation during nongrowing season months is particularly effective at recharging the moisture of the deeper soil layers, thus differentially promoting the growth of the deeper rooted trees over grasses. Increased tree leaf biomass reduced light availability in the understory, which constrained grass growth and increased the moisture and nutrients available to trees.

The biomass of both trees and grass (Figure 8) increased under the HadCM2 scenario as a response to increased precipitation in the southern half of the Great Central Valley and in the highlands of the Mojave Desert. The increase in total vegetation biomass (Figure 7b), and especially the increase in grass biomass, produced more fire (i.e., shorter mean fire rotation periods, Figure 9a) and higher fire intensity (Figure 9b). A relatively small area of tree carbon decline was simulated under the HadCM2 scenario, and the decline was located primarily in the most arid portion of the state in the Sonoran Desert and the lowlands of the Mojave Desert (Figure 8a). Here greater grass biomass (Figure 8b) supported by increased precipitation also produced more frequent and extreme fire (Figures 9a,b), which helped constrain woody biomass.

The simulated trend in percentage of area burned under the HadCM2 scenario (Figure 16a) was more variable than the simulated historical trend (coefficients of variation were 21% and 15%). The increase in precipitation under the HadCM2 scenario served to increase the variability of the fire regime by reducing area burned to lower levels and contributing to greater biomass buildup during the relatively wet years, thus setting the system up for higher levels of burned area promoted by higher fuel loads during the relatively dry years. This interaction between fuels and interannual variability in precipitation produced the somewhat counterintuitive result of more severe fire years simulated under the wetter HadCM2 scenario. The model predicts three fire events (in 2027, 2044, and 2074) under the HadCM2 scenario (Figure 16a) that are more severe than any event simulated for the historical period (Figure 10). The smoothed trend in simulated percentage of area burned for the HadCM2 scenario (Figure 16b) shows a distinct rise above the simulated historical mean in the last few decades of the future period. However, linear regression analysis showed that, overall, the slope of the HadCM2 trend was not significantly different than zero.

3.2.2.2 Parallel climate model scenario

In contrast to the response under the HadCM2 scenario, there was a widespread decrease in tree carbon density (Figure 8a) in response to the decrease in total annual precipitation under the PCM scenario. The reduction in deep soil moisture recharge shifted the competitive advantage to

A.

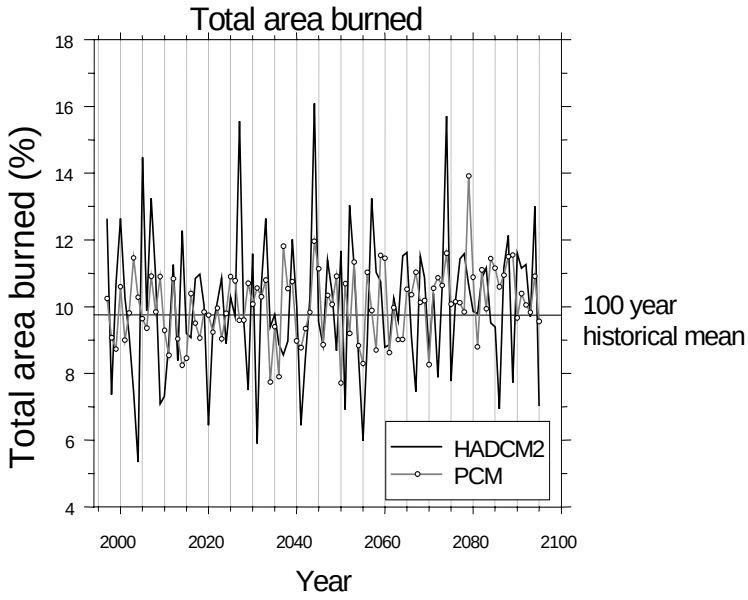

B.

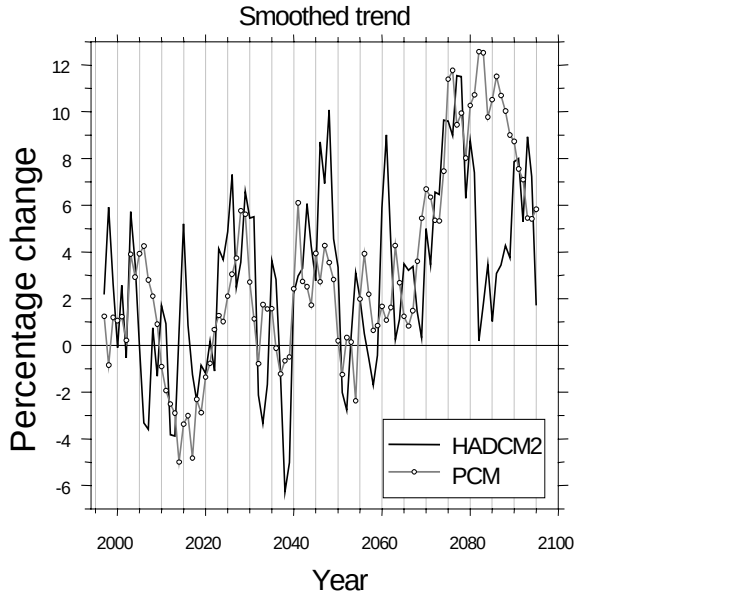

Figure 16. Simulated trends in (a) the annual percentage of the total area burned and (b) the smoothed percentage deviation from the 100 year historical mean for the future period (1994-2099) of the HadCM2 and PCM climate scenarios

grasses, producing a widespread increase in grass biomass (Figure 8b) that was strongly related to the decline in tree biomass. Fire frequency increased (Figure 9a) where the increase in grass biomass was greatest, and fire intensity increased (Figure 9b) where the net result of increased grass and decreased tree biomass was a gain in total vegetation biomass (Figure 7b).

Two exceptions to this widespread response to the PCM scenario were along the coast and along the Sierra Nevada where the biomass of trees increased and grasses declined (Figures 8). In these relatively cool parts of the state, simulated tree growth was restricted by temperature as well as moisture availability. Decreases in precipitation were relatively small under the PCM scenario (Figure 4b) in these two regions. Here increased temperatures without significant changes in moisture availability promoted increased tree growth and corresponding declines in grass growth. The decline in grass biomass produced a reduction in fire frequency along the coast where it was already very low in the historical simulation (Figure 9a). In fact, fire frequency dropped to zero or near zero along much of the coast under this scenario, producing the large percentage changes in fire intensity (Figure 9b).

The most arid portion of the state (the Sonoran Desert and Mojave Desert lowlands) was the other region where an exception was seen to the general trend of increased grass biomass and decreased tree biomass under the PCM scenario. Here tree and grass biomass both declined (Figure 8). In this same region, the largest increases in annual temperature (Figure 4a) and the largest decreases in annual precipitation (Figure 4b) were predicted under the PCM scenario. The response to the decrease in effective moisture was a decrease in total vegetation biomass and attendant decreases in measures of simulated fire activity (Figure 9).

The simulated trend in percentage of area burned under the PCM scenario (Figure 16a) was less variable than the simulated historical trend (coefficients of variation were 10% and 15%). The smoothed trend in simulated percentage of area burned for the PCM climate scenario (Figure 16b) shows a distinct rise above the simulated historical mean in the last few decades of the future period, and linear regression analysis showed that the slope of the PCM trend was significantly different than zero.

3.2.3 Future carbon budget

Simulated total ecosystem carbon for the entire state increases at a fairly steady and nearly equal rate under both future climate scenarios (Figure 17a). An increase of about 6% over the size of the historical pool is simulated at the end of the 21st century under both scenarios (Table 3). The rate and size of the increase in total ecosystem carbon under each scenario is largely driven by the simulated future trends in the soil and litter carbon pool (Figure 17b) which comprises over 90% of the total carbon pool (Table 3). The total live vegetation pool (Figure 17c) also shows a similar rate of increase under both scenarios throughout much of the future period. However, this

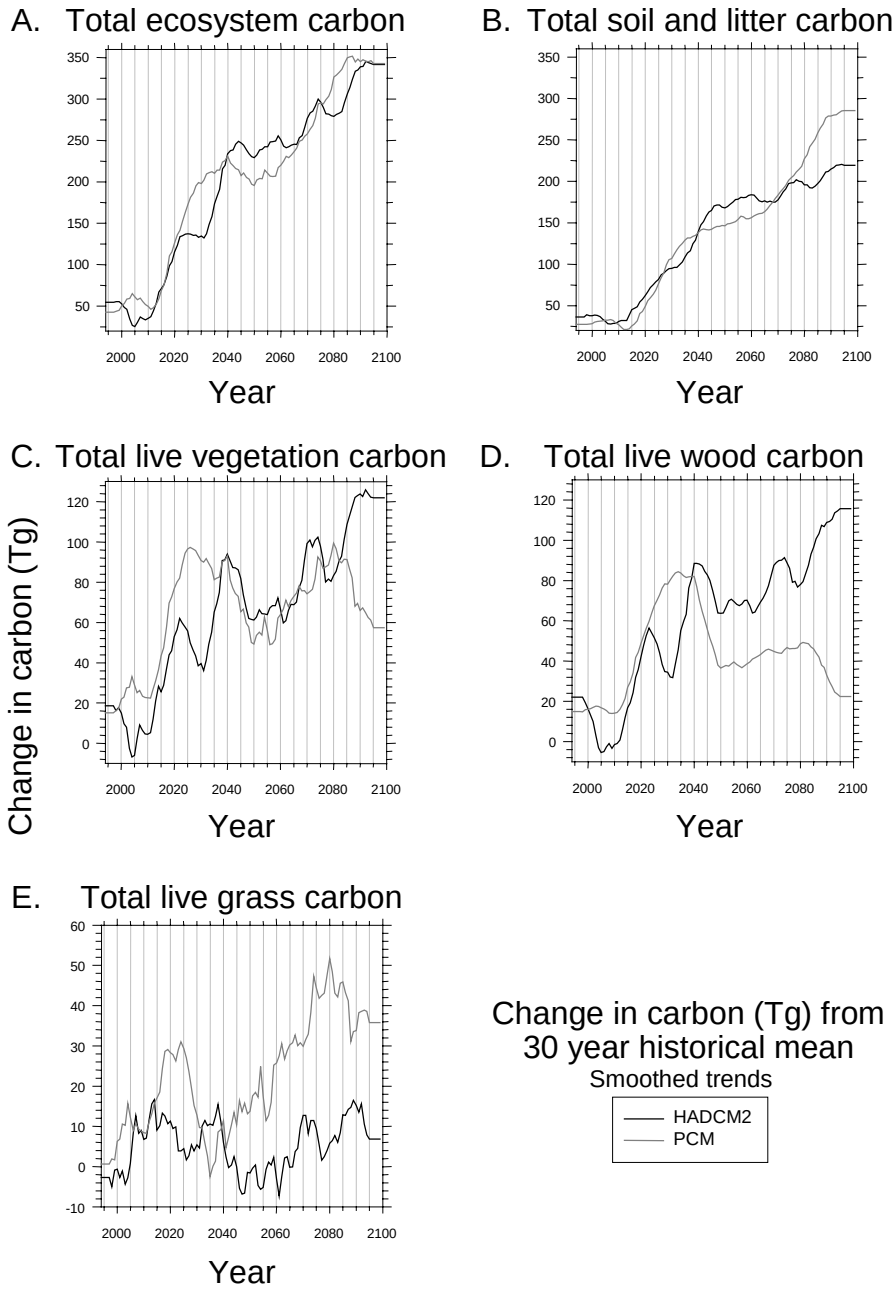

Figure 17. Percentage changes simulated for storage in different carbon pools (a-e) under the HadCM2 and PCM scenarios. Changes are for the future period (2070-2099) relative to the historical period (1961-1990). Trends were smoothed for display using a 10 year running average.

Table 3. Size of the historical carbon pools simulated for the state of California and future changes in size simulated under the HadCM2 and PCM climate scenarios[a]

Carbon pool	HIST (Tg)	HadCM2 change (Tg)	PCM change (Tg)
Total ecosystem	5765	+312	+325
Soil and litter	5305	+203	+246
Total live vegetation	461	+107	+78
Live wood	300	+99	+38
Live grass	163	+9	+41

a. HIST values in teragrams are the mean weights for the 30 year (1961-1990) base period. HadCM2 and PCM change values in teragrams are the mean weights for the 30 year (2070-2099) future period subtracted from the mean weights for the historical period.

similarity is the net result of different responses to the two scenarios by the wood and grass components of the total vegetation carbon pool. The wood component (Figure 17d) is the primary contributor to the increase in total vegetation carbon under the wetter HadCM2 scenario. The grass component is a greater contributor to the increase under the drier PCM scenario (Figure 17e).

The common response under both climate scenarios was an increase in statewide carbon storage produced by temperature-driven increases in productivity. Fluctuations in vegetation carbon storage (Figure 17c) showed a marked correspondence to fluctuations in future total annual precipitation under each scenario (Figure 2b). However, the total amount of vegetation carbon storage was comparable under the each scenario throughout much of the future simulation period, despite the disparate trends in precipitation. Up until the last couple of decades of the simulation period, the simulated response to the increasingly wetter HadCM2 (or increasingly drier PCM) scenario was an increased proportion of the total vegetation carbon stored as wood (or grass) carbon (Figure 17d,e). A precipitation effect on the trend of total vegetation carbon pool is clearly evident only near the end of the future period, when the two scenarios are most distinct in terms of total annual precipitation (Figure 2b). At about 2085, the live vegetation carbon pool declined under the drier PCM scenario but continued to increase under the wetter HadCM2 scenario (Figure 17c). The decline in live vegetation carbon under the PCM scenario is the net result of declines in both the wood (Figure 17d) and grass (Figure 17e) carbon pools. Despite this decline in vegetation carbon, total ecosystem carbon under the PCM scenario (Figure 17a) was relatively unaffected because of a compensating increase in soil and litter carbon (Figure 17b). The increase in the latter is apparently a lagged effect of the relatively steep increase in grass carbon just before the period of vegetation carbon decline under the PCM scenario (Figure 17e). Grass carbon is an especially effective contributor to soil carbon in the model because of the fast turnover rate and because a large proportion of grass biomass is below ground and protected from consumption by fire.

4. Conclusions

The MC1 simulation for the historical climate of California appeared to achieve a reliable level of prediction, although validating a broad-scale model of potential vegetation presents numerous difficulties. The simulation of the coverage and distribution of vegetation classes was largely in agreement with the baseline vegetation map developed from the Küchler (1975) map of potential vegetation, and some of the discrepancies between the two were likely attributable to lack of detail in the Küchler map. The model also appeared to accurately simulate the relative distribution of tree and grass carbon, and average values of the simulated total vegetation carbon per vegetation class were largely in agreement with published values for equivalent classes. The simulated mean fire return intervals fell within the range of independent estimates of fire frequency in different vegetation types, and simulated fire intensities conformed to those expected for severe fire in different vegetation classes. Most of the severe fire years simulated by the model were coincident with observed drought years, and with observed severe fire years in the historical record for U.S. Forest Service land in California.

More rigorous validation of the simulation results for the historical climate was difficult given the nature of the simulations. The model simulates dynamic ecosystem properties only as a function of climate and soils, and does not include the effects of land use practices. The extent to which the natural ecosystems of California have been modified by land use can be partially demonstrated by masking out areas of agriculture and urbanization on the vegetation class map simulated for the historical climate (Figure 5c). This is a conservative view of the impact of land use in the state given the relatively coarse scale of the mask and the unrepresentative impact of forestry and grazing on the unmasked areas. The impact of the latter includes modifications to life form mixtures, carbon stocks, and fire regimes. Also, the model does not include lags in vegetation change caused by migration and dispersal over a landscape fragmented by land use practices. Ongoing efforts to incorporate land use effects in MC1 and to increase the spatial resolution of the model simulations should increase the realism of the model results and facilitate their validation against observed data from the extant landscape.

Compounding the uncertainty arising from the model's limitations are the existence of a large number of GCM-generated global climate change scenarios that could be used to construct regional-scale scenarios for California. In a recent analysis, the California portions of more than 20 GCM simulations were examined to ascertain any consistent projections of climate change (T. Wrigley, NCAR, personal communication, January 11, 2001). All the models estimated warmer temperatures for the state, but there was much less consistency regarding precipitation. The models ranged from estimating a 56% increase to a 10% decrease in winter precipitation, with about two-thirds of the models estimating an increase in winter precipitation. The average change in summer precipitation was near zero. The conclusion was that California is likely to be warmer and probably wetter during the winter months. The HadCM2 scenario represents this

well. However, none of the available scenarios should be interpreted as predictions of climate change in California. Their proper use is in the investigation of the sensitivities of natural and managed systems to potential changes in climate.

The results of the MC1 simulations for California demonstrate certain ecosystem sensitivities and interactions that are likely to be features of the response of both natural and seminatural (e.g., managed forests and rangelands) systems to the relatively certain rise in temperature and the less certain changes in precipitation. The most widespread response to the increase in temperature under both scenarios was a shift from conifer-dominated forests to mixed forests of conifers and evergreen hardwoods, primarily in the mountainous areas of the northern half of the state. Warmer temperatures increased the competitiveness of the evergreen hardwoods, which are less tolerant of low winter temperatures than conifers (Woodward, 1987). Higher temperatures also increased tree productivity in areas along the north-central coast and at high elevations where water stress is relatively low and growing season warmth is a constraint on growth. For example, currently the highest monthly mean temperatures along the north-central coast (e.g., 14.6°C, 13.5°C, and 16.8°C at Crescent City, Point Reyes, and Monterey, respectively; Major, 1995) are below the mean summer temperature for optimal coast redwood forest productivity (17.8°C; Kuser, 1976) and below the optimum temperature for redwood seedling growth (18.9°C; Hellmers and Sundahl, 1959). However, increased forest productivity with increased growing season temperature along the north-central coast would be contingent on the persistence of summer fog, which provides more than 30% of the annual soil moisture (Dawson, 1998). If increased temperatures were accompanied by a major decrease in coastal fog, the increased moisture stress would result in a decline in productivity or even the elimination of coast redwood forest and associated maritime forest types.

The simulated responses to changes in precipitation under the two future climate scenarios were more complex, involving not only a direct effect on vegetation productivity associated with changes in available soil moisture, but also changes in tree-grass competition that were mediated by fire. The persistence of a Mediterranean climate with dry summers was a key feature of the modeled response. Under the HadCM2 scenario, increased winter precipitation favored the more deeply rooted trees overall. More winter precipitation (together with CO_2-induced increases in water use efficiency) produced increases in tree carbon density sufficient to replace shrubland and woodland with forest in relatively mesic areas of the state. But in the more semiarid regions, where annual precipitation continued to support codominance of trees and grasses, increased fire promoted by greater biomass and the persistently dry summers favored grasses, which recovered from fire-induced reductions in biomass more rapidly than trees. Consequently, under the HadCM2 scenario, increases were seen in both the forest cover at the expense of woodland and shrubland and the productivity of grasslands.

Declines in winter precipitation under the PCM scenario produced a very different modeled response. A widespread decrease in tree carbon density increased the light, moisture, and nutrients available to the more drought-resistant grasses. The decrease in tree carbon density was not sufficient to convert much forested area to woodland or shrubland. But in the more ecotonal areas, increased grass biomass resulting from reduced competition with trees promoted more fire during the persistently dry summers, converting shrubland and woodland to grassland. Consequently, under the PCM scenario, there was an increase in the coverage of grassland at the expense of woodland and shrubland and a decrease in the productivity of forests.

Fire was a critical element in the simulated response to both future climate scenarios. The summer months were warmer and persistently dry under both scenarios, so differences in the modeled fire behavior and effects were primarily a response to differences in simulated fuels. The modeled extent of fire was most sensitive to changes in grass biomass. Changes in grass biomass produced changes in fuel loading and fuel bed structure that are strong determinants of the rate of fire spread simulated by the model. Increases in grass biomass were projected for different regions of the state under the HadCM2 and PCM scenarios, so the regions of simulated increases in fire area were also distinct. The simulated intensity of fire is more sensitive to the total amount of vegetation (i.e., tree and grass) carbon available for consumption. Different ratios of tree and grass carbon produced similar levels of total vegetation carbon under the two scenarios, resulting in a greater degree of overlap for regions of increased fire intensity than for regions of increased fire area.

Although neither of the model simulations for the two climate scenarios should be taken as predictions of the future, it is evident from the results that all the natural ecosystems of California, whether managed or unmanaged, are likely to be affected by changes in climate. Changes in temperature and precipitation will alter the structure, composition, and productivity of vegetation communities, and wildfires may become more frequent and intense. The incidence of pest outbreaks in forests stressed by a changing climate could act as a positive feedback on the frequency and intensity of fire. Non-native species that are preadapted to disturbance could colonize altered sites in advance of native species, preventing the already problematical redistribution of natives across a landscape highly fragmented by land use practices. Both plants and animals already stressed by human development will be further stressed by climate change. Some may not be able to adapt, and the number of threatened and endangered species could rise significantly. Tree species better adapted to a changed climate could be planted in forests managed for wood production, but better adapted species may not have the same market value (e.g., conifer species versus hardwood species). The expansion of grasslands under a drier climate might benefit grazing livestock, but any gains might be offset by decreased water availability.

Considerable uncertainty exists with respect to regional-scale impacts of global warming. Much of this uncertainty resides in the differences among the different GCM climate scenarios as illustrated in this study. In addition, models that translate climatic scenarios into projections of ecosystem impacts can always be improved through re-examination and improvement of model processes. Nevertheless, the results of this study underscore the potentially large impact of climate change on California ecosystems, and the need for further use and development of dynamic vegetation models using various ensembles of climate change scenarios.

Acknowledgments

We would like to thank the Electric Power Research Institute and the California Energy Commission for project support. We would also like to thank Christopher Daly of the Spatial Climate Analysis Service at Oregon State University for supplying spatially distributed, historical climate data, and Aiguo Dai of NCAR's Climate Analysis Section for providing the PCM future climate scenario.

References

Aber, J., R.P. Neilson, S. McNulty, J.M. Lenihan, D. Bachelet, and R.J. Drapek. 2001. Forest processes and global environmental change: Predicting the effects of individual and multiple stressors. *Bioscience* 51(9):735-751.

Atjay, G., P. Ketner, and P. Duvigneaud. 1979. Terrestrial primary production and phytomass. In *The Global Carbon Cycle*, B. Bolin, E. Degens, S. Kempe, and P. Ketner (eds.). John Wiley and Sons, New York. pp. 129-182.

Bachelet, D., J. Lenihan, C. Daly, and R. Neilson. 2000. Interactions between fire, grazing and climate change at Wind Cave National Park, SD. *Ecological Modelling* 134:219-224.

Bachelet, D., R.P. Neilson, J.M. Lenihan, and R.J. Drapek. 2001a. Climate change effects on vegetation distribution and carbon budget in the U.S. *Ecosystems* 4:164-185.

Bachelet, D., J. Lenihan, C. Daly, R. Neilson, D. Ojima, and W. Parton. 2001b. MC1: A Dynamic Vegetation Model for Estimating the Distribution of Vegetation and Associated Ecosystem Fluxes of Carbon, Nutrients, and Water. General Technical Report PNW-GTR-508. USDA Forest Service, Pacific Northwest Research Station, Portland, OR.

Barbour, M., B. Pavlik, F. Drysdale, and S. Lindstrom. 1993. *California's Changing Landscapes: Diversity and Conservation of California Vegetation*. California Native Plant Society, Sacramento. 246 pp.

California Division of Tourism. 2001. Visitor statistics. Available at http://gocalif.ca.gov/research/visitor.html.

Dai, A., G.A. Meehl, W.M. Washington, T.M.L. Wigley, and J.A. Arblaster. 2001. Ensemble simulation of 21st century climate changes: Business as usual versus CO_2 stabilization. *Bulletin of the American Meteorology Society* 82:2377-2388.

Daly, C., R.P. Neilson, and D.L. Phillips. 1994. A statistical-topographic model for mapping climatological precipitation over mountainous terrain. *Journal of Applied Meteorology* 33:140-158.

Daly, C., D. Bachelet, J. Lenihan, W. Parton, R. Neilson, and D. Ojima. 2000. Dynamic simulations of tree-grass interactions for global change studies. *Ecological Applications* 10:449-469.

D'Antonio, C.M. and P.M. Vitousek. 1992. Biological invasions by exotic grasses, the grass/fire cycle, and global change. *Annual Review of Ecology and Systematics* 23:63-87.

Davis, F.W., D.M. Stoms, A.D. Hollander, K.A. Thomas, P.A. Stine, D. Odion, M.I. Borchert, J.H. Thorne, M.V. Gray, R.E. Walker, K. Warner, and J. Graae. 1998. The California Gap Analysis Project, Final Report. University of California, Santa Barbara.

Dawson, T. 1998. Fog in the California redwood forest: Ecosystem inputs and use by plants. *Oecologia* 117:476-485.

Field, C., G. Daily, F. Davis, S. Gaines, P. Matson, J. Melack, and N. Miller. 1999. Confronting Change in California: Ecological Impacts on the Golden State. Report of the Union of Concerned Scientists and the Ecological Society of America. UCS Publications, Cambridge, MA.

Gutowski, W.J., Z. Pan, C.J. Anderson, R.W. Arritt, F. Otieno, E.S. Takle, J.H. Christensen, and O.B. Christensen. 2000. What RCM Data are Available for California Impacts Modeling? California Energy Commission Workshop on Climate Change Scenarios for California, California Energy Commission, Sacramento, 12-13 June.

Heinselman, M. 1973. Fire in the virgin forests of the Boundary Waters Canoe Area, Minnesota. *Quaternary Research* 3:329-328.

Hickman, J.C. 1993. *The Jepson Manual: Higher Plants of California*. University of California Press, Berkeley.

Holland, V. and D. Keil. 1995. *California Vegetation.* Kendall/Hunt Publishing Company, Dubuque, IA.

Houghton, R. and J. Hackler. 2000. Changes in terrestrial carbon storage in the United States. 1: The roles of agriculture and forestry. *Global Ecology and Biogeogra*phy 9:125-144.

Husari, S. and K. McKelvey. 1996. Fire-Management Policies and Programs. In *Sierra Nevada Ecosystem Project: Final Report to Congress. Vol. II: Assessments and Scientific Basis for Management Options,* F. Davis (ed.). University of California Centers for Water and Wildland Resources Report 36, Davis. pp. 1101-1117.

Jensen, D., M. Torn, and J. Harte. 1993. *In Our Own Hands – A Strategy for Conserving California's Biological Diversity*. University of California Press, Berkeley.

Karl, T.R. 1986. The sensitivity of the Palmer Drought Severity Index and Palmer's Z-Index to their calibration coefficients including potential evapotranspiration. *Journal of Climate and Applied Meteorology* 25:77-86.

Kattenberg, A., F. Giorgi, H. Grassl, G. Meehl, J. Mitchell, R. Stouffer, T. Tokioka, A. Weaver, and T. Wigley. 1996. Climate models: projections of future climate. In *Climate Change 1995: The Science of Climate Change. Contribution to Working Group 1 to the Second Assessment Report of the Intergovernmental Panel on Climate Change,* J. Houghton, L. Meira Filho, B. Callander, N. Harris, A. Kattenberg, and K. Maskell (eds.). Cambridge University Press, Cambridge, UK. pp. 285-357.

Keane, R., C. Hardy, and K. Ryan. 1997. Simulating effects of fire on gaseous emissions and atmospheric carbon fluxes from coniferous forest landscapes. *World Resource Review* 9(2):177-205.

Kittel, T.G.F., J.A. Royle, C. Daly, N.A. Rosenbloom, W.P. Gibson, H.H. Fisher, D.S. Schimel, L.M. Berliner, and VEMAP2 Participants. 1997. A gridded historical (1895-1993) bioclimatic dataset for the conterminous United States. In *Proceedings of the 10th Conference on Applied Climatology, 20-24 October 1997, Reno, NV.* American Meteorological Society, Boston. pp. 219-222.

Küchler, A. 1975. Potential natural vegetation of the United States. 2nd ed. Map 1:3,168,000. American Geographic Society, New York.

Kuser, J. 1976. The site quality of redwood. MS thesis. Rutgers University, New Brunswick, NJ.

Lenihan, J.M., C. Daly, D. Bachelet, and R.P. Neilson. 1997. Simulating broad-scale fire severity in a dynamic global vegetation model. *Northwest Science* 72:91-103.

Lertzman, K., J. Fall, and B. Dorner. 1998. Three kinds of heterogeneity in fire regimes: At the crossroads of fire history and landscape ecology. *Northwest Science* 72 (Special Issue):4-23.

Major, J. 1995. California climate in relation to vegetation. In *Terrestrial Vegetation of California,* M. Barbour and J. Major (eds.). California Native Plant Society Special Publication No. 9. Fourth CNPS Printing, Sacramento. pp. 11-74.

Martin, R. and D. Sapsis. 1995. A synopsis of large or disastrous wildlands fires. In *The Biswell Symposium: Fire Issues and Solutions in Urban Interface and Wildland Ecosystems,* D. Weise and R. Martin (technical coordinators). General Technical Report PSW-GTR-158. USDA Forest Service Pacific Southwest Research Station, Albany, CA. pp. 15-17.

McKelvey, K. and K. Busse. 1996. Twentieth-century fire patterns on Forest Service lands. In *Sierra Nevada Ecosystem Project: Final Report to Congress. Volume II: Assessments and Scientific Basis for Management Options,* F. Davis (ed.). University of California Centers for Water and Wildland Resources Report 36, Davis. pp. 1119-1138.

Mitchell, J.F.B. and T.C. Johns. 1997. On modification of global warming by sulphate aerosols. *Journal of Climate* 10(2):245-267.

National Assessment Synthesis Team (eds.). 2001. *Climate Change Impacts on the United States: Foundation Report.* U.S. Global Change Research Program. Cambridge University Press, New York.

Neilson, R. 1995. A model for predicting continental-scale vegetation distribution and water balance. *Ecological Applications* 5(2):362-385.

Parton, W., D. Schimel, D. Ojima, and C. Cole. 1994. A general study model for soil organic model dynamics, sensitivity to litter chemistry, texture, and management. SSSA Special Publication 39. *Soil Science Society of America* 147-167.

Peterson, D. and K. Ryan. 1986. Modeling postfire conifer mortality for long-range planning. *Environmental Management* 10:797-808.

Rothermel, R. 1972. A mathematical model for fire spread predictions in wildland fuels. USDA Forest Service Research Paper INT-115. USDA Forest Service, Intermountain Forest and Range Experiment Station, Ogden, UT.

Rothermel, R. 1983. How to Predict the Spread and Intensity of Forest and Range Fires. General Technical Report INT-143. USDA Forest Service, Intermountain Forest and Range Experiment Station, Ogden, UT.

Sawyer, J., D. Thornburg, and J. Griffin. 1995. Mixed evergreen forest. In *Terrestrial Vegetation of California,* M. Barbour and J. Major (eds.). California Native Plant Society Special Publication No. 9, Fourth CNPS Printing, Sacramento. pp. 359-382.

Scheffer, M., S. Carpenter, J. Foley, C. Folke, and B. Walker. 2001. Catastrophic shifts in ecosystems. *Nature* 413:591-596.

Skinner, C. and C. Chang. 1996. Fire regimes, past and present. In *Sierra Nevada Ecosystem Project: Final Report to Congress. Vol. II: Assessments and Scientific Basis for Management Options,* F. Davis (ed.). University of California Centers for Water and Wildland Resources Report 36, Davis, CA. pp. 1041-1069.

Strauss, D., L. Bednar, and R. Mees. 1989. Do one percent of forest fires cause ninety-nine percent of the damage? *Forest Science* 35:319-328.

Swetnam, T. and J. Betancourt. 1998. Mesoscale disturbance and ecological response to decadal climatic variability in the American Southwest. *Journal of Climate* 11:3128-3142.

Turner, M. and W. Romme. 1994. Landscape dynamics in crown fire ecosystems. *Landscape Ecology* 9(1):59-77.

U.S. Fish and Wildlife Service. 2001. Number of listed species in each state or territory. Available at http://ecos.fws.gov/webpage/usmap.html?&status = listed.

van Wagner, C.E. 1993. Prediction of crown fire behavior in two stands of jack pine. *Canadian Journal of Forest Research* 23:442-449.

Vogel, R., W. Armstrong, K. White, and K. Cole. 1995. The closed-cone pines and cypresses. In *Terrestrial Vegetation of California,* M. Barbour and J. Major (eds.). California Native Plant Society Special Publication No. 9, Fourth CNPS Printing, Sacramento. pp. 295-358.

Wilkinson, R. and T. Rounds. 1998. Climate Change and Variability in California: White Paper for the California Regional Assessment. National Center for Ecological Analysis and Synthesis, Santa Barbara, CA.

Woodward, F. 1987. *Climate and Plant Distribution*. Cambridge University Press, New York.

Appendix IV — Attachment

The Simulated Ecosystem Response to the Incremental Future Climate Scenarios

A.1 Incremental Future Climate Scenarios

Four incremental scenarios of future temperature and precipitation change (Table A.1) were developed to represent more intermediate changes in climate than were represented by the HadCM2 and PCM climate scenarios. Two temperature change scenarios were selected to represent a 3.0°C and 5.0°C rise in temperature by the end of the 21st century. The 3.0°C change is consistent with a global average warming of 2.5°C, which is considered to be the most likely climate change by 2100 (T. Wigley, NCAR, personal communication, January 11, 2001). GCMs show that, on average, California will warm 14% more than the global average climate, yielding an increase of about 3°C.

Two precipitation change scenarios were selected for implementation in conjunction with the temperature scenarios. A "no change" scenario was selected because the average change in summer precipitation across GCM experiments is around zero for California (T. Wigley, NCAR, personal communication, January 11, 2001). The second scenario assumes a 6% increase in precipitation per degree Celsius of warming, which corresponds with the average GCM change in winter precipitation per degree Celsius warming in California (T. Wigley, NCAR, personal communication, January 11, 2001).

Time series of monthly precipitation and temperature for the period from 1994 to 2100 were developed for each incremental scenario by applying accumulating increments to a foundation of detrended monthly temperature and precipitation time-series data. The detrended time series were developed from the spatially distributed historical (1895-1993) climate time series for California. Because both the historical temperature and the precipitation time series showed increasing trends over time, it was necessary to use the detrended series as the foundation for the

Table A.1. Incremental climate scenario designations and increases in mean annual temperature and total annual precipitation at the end of the 21st century

Incremental scenario	Increase in temperature (°C)	Increase in precipitation (%)
T3P0	+3	0
T3P18	+3	18
T5P0	+5	0
T5P30	+5	30

future scenarios to avoid step changes from the end of the historical period to the beginning of the future scenario period. Also, because the detrended time series were developed previously for the purpose of model simulation "spinup," mean monthly values from the beginning (not the end) of the historical period were used in the detrending process. So, for the purposes of their use as a foundation for the incremental scenarios, it was necessary to adjust the mean level of the detrended time series to avoid another step change from 1993 to 1994. An adjustment factor was calculated (at each grid cell) as the difference between the mean of the monthly temperatures (or monthly precipitation values) over the last 30 years of the historical time series and the mean of the same over the entire detrended historical time series. This adjustment factor was added to each value in the detrended historical time series to create a foundation time series for the future scenario time series. And because each of the adjusted, detrended historical time series was only 100 years long, it was necessary to the repeat the first 7 years at the end to create the 107 year (1994-2100) foundation time series for the future climate scenarios.

The final step in creating the incremental scenarios was adding accumulating increments of temperature or precipitation to each monthly value in the foundation time series. The accumulated increment for a given month was calculated as the specified final increment at the end of the future scenario period divided by the number of months in the future scenario, and then multiplied by the serial rank of the given month. For example, if the specified final temperature increment was 3°C, and the monthly temperature value for the month halfway through the foundation time series (i.e., month 642 out of the total 1,284 months for the 107 year period) was 30°C, the scenario value for that month would be calculated as ((3/1284) * 642) + 30 = 31.5°C.

The trends in mean annual temperature show a nearly monotonic rise under the T3 and T5 incremental temperature scenarios (Figure A.1). Total annual precipitation under the P18 and P30 incremental precipitation scenarios is more variable, showing periods of both increase and decline. This interannual variation in precipitation is that of the underlying foundation time series (i.e., the adjusted, detrended historical time series for total monthly precipitation) used to develop the incremental precipitation scenarios.

A.2 Response of the Vegetation Classes to Incremental Scenarios

The response of vegetation class distribution under the incremental scenarios was determined by comparing the most frequent vegetation type simulated at each grid cell for the 30 year historical period (1961-1990) against the same for the last 30 years (2071-2100) of the incremental scenarios (Figures A.2-A.4).

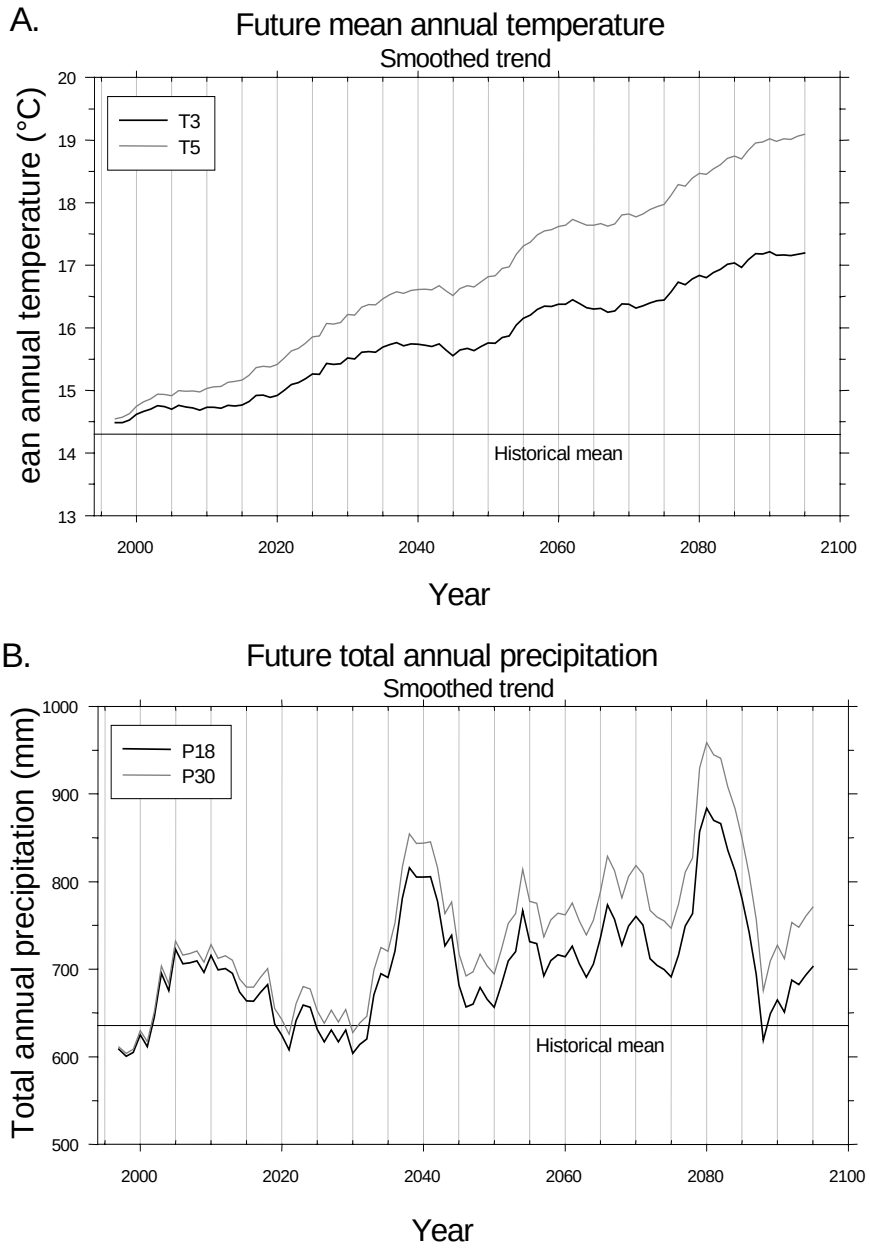

Figure A.1. Future trends in (a) mean annual temperature and (b) total annual precipitation under the incremental climate scenarios. Annual values are averages across all grid cells. Trends were smoothed for display using a 10 year running average.

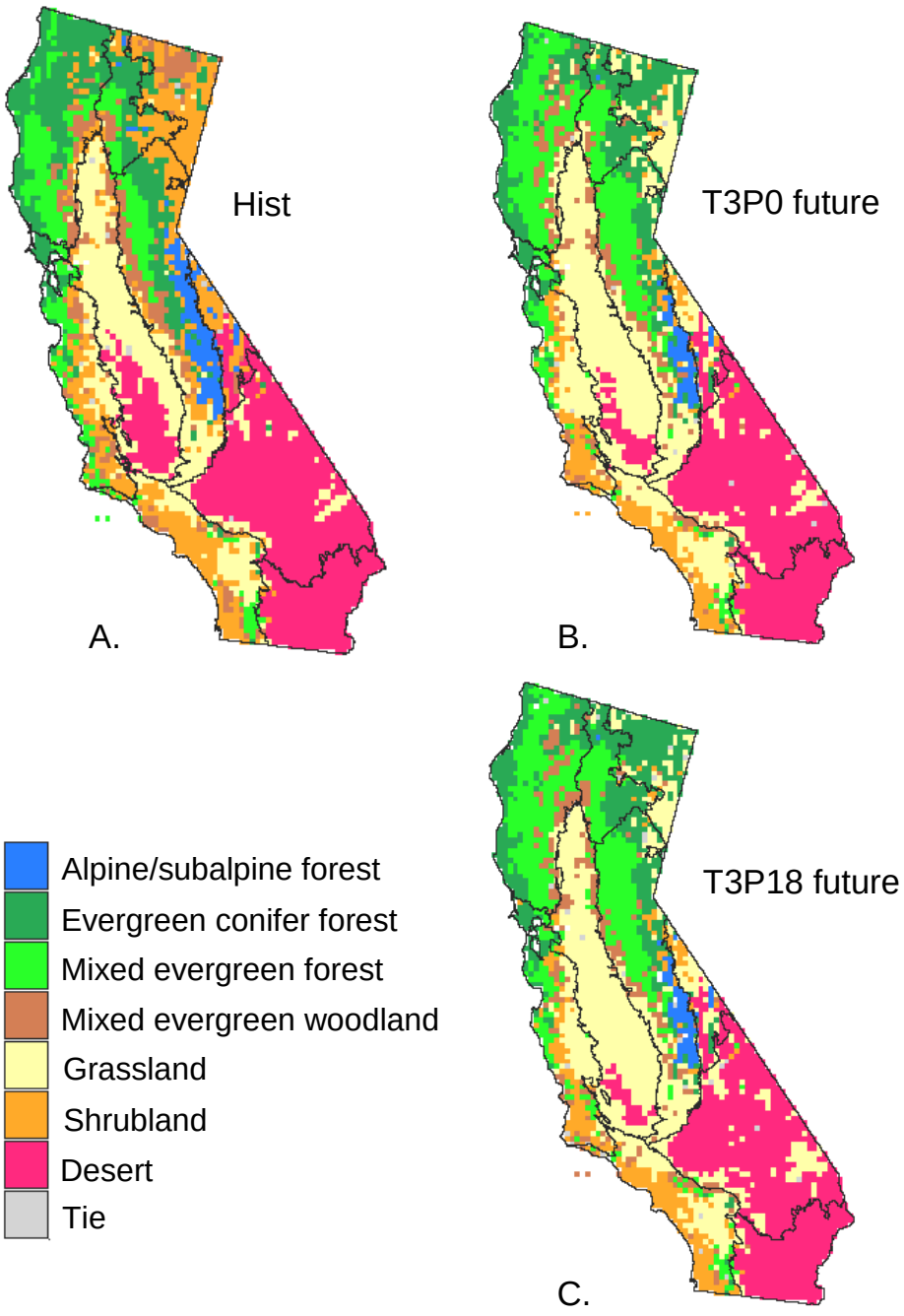

Figure A.2. Distribution of the vegetation classes simulated for (a) the historical period (1961-1990), and (b,c) the 30 year future period (2070-2099) of the T3 incremental climate scenarios. The vegetation class mapped at each grid cell in is the most frequent class simulated during the time period. A "tie" is where two or more classes were equally frequent.

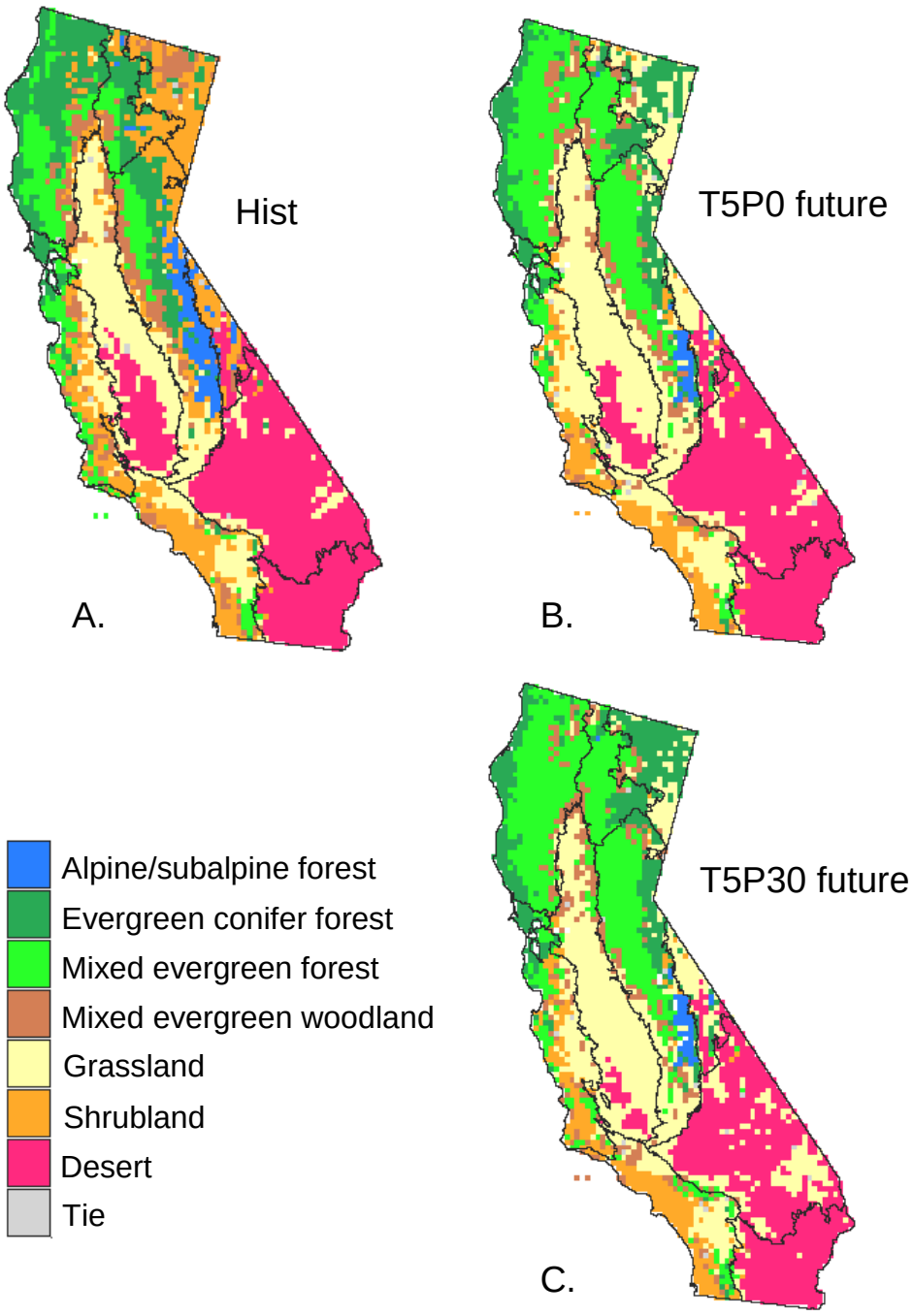

Figure A.3. Distribution of the vegetation classes simulated for (a) the historical period (1961-1990), and (b,c) the 30 year future period (2070-2099) of the T5 incremental climate scenarios

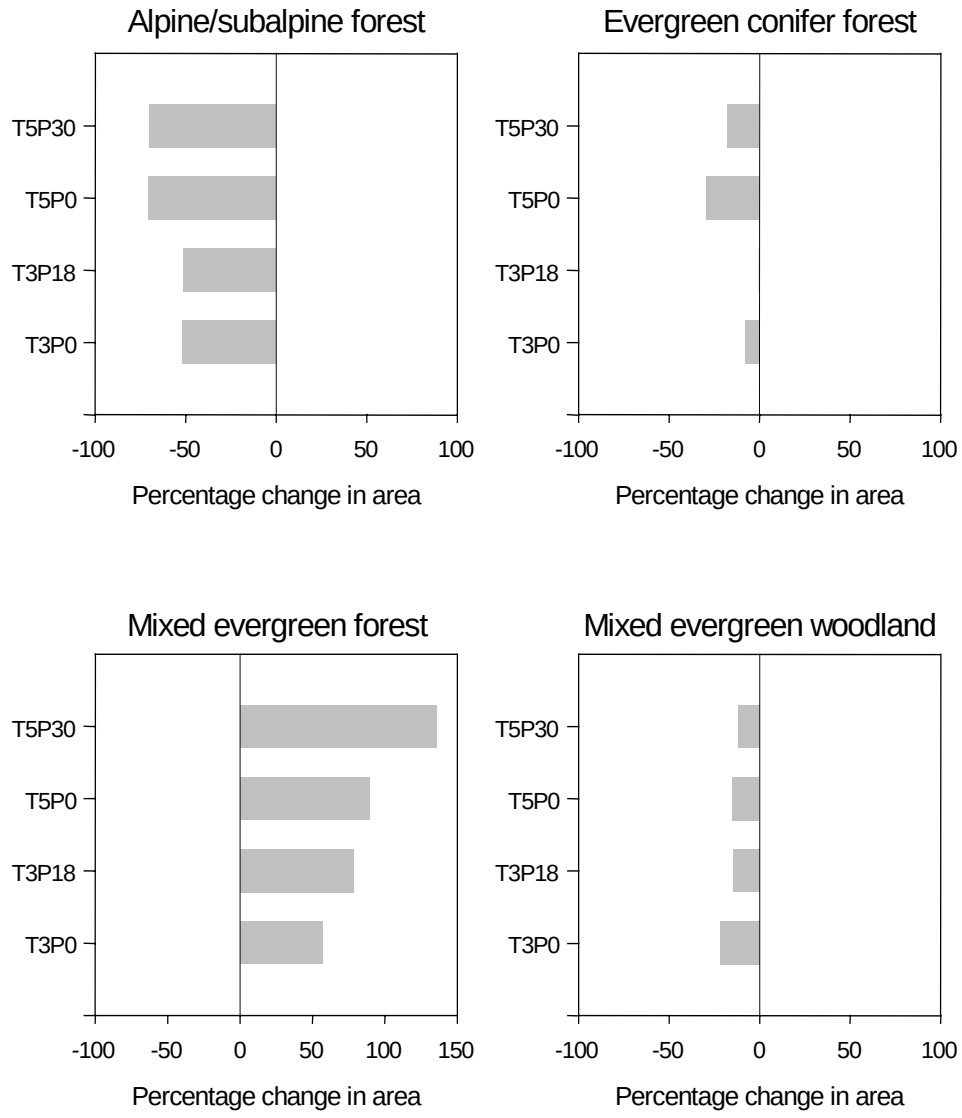

Figure A.4. Percent changes in the simulated total cover of the vegetation classes under the incremental climate scenarios. Changes were calculated for the 30 year future period (2070-2099) relative to the historical period (1961-1990).

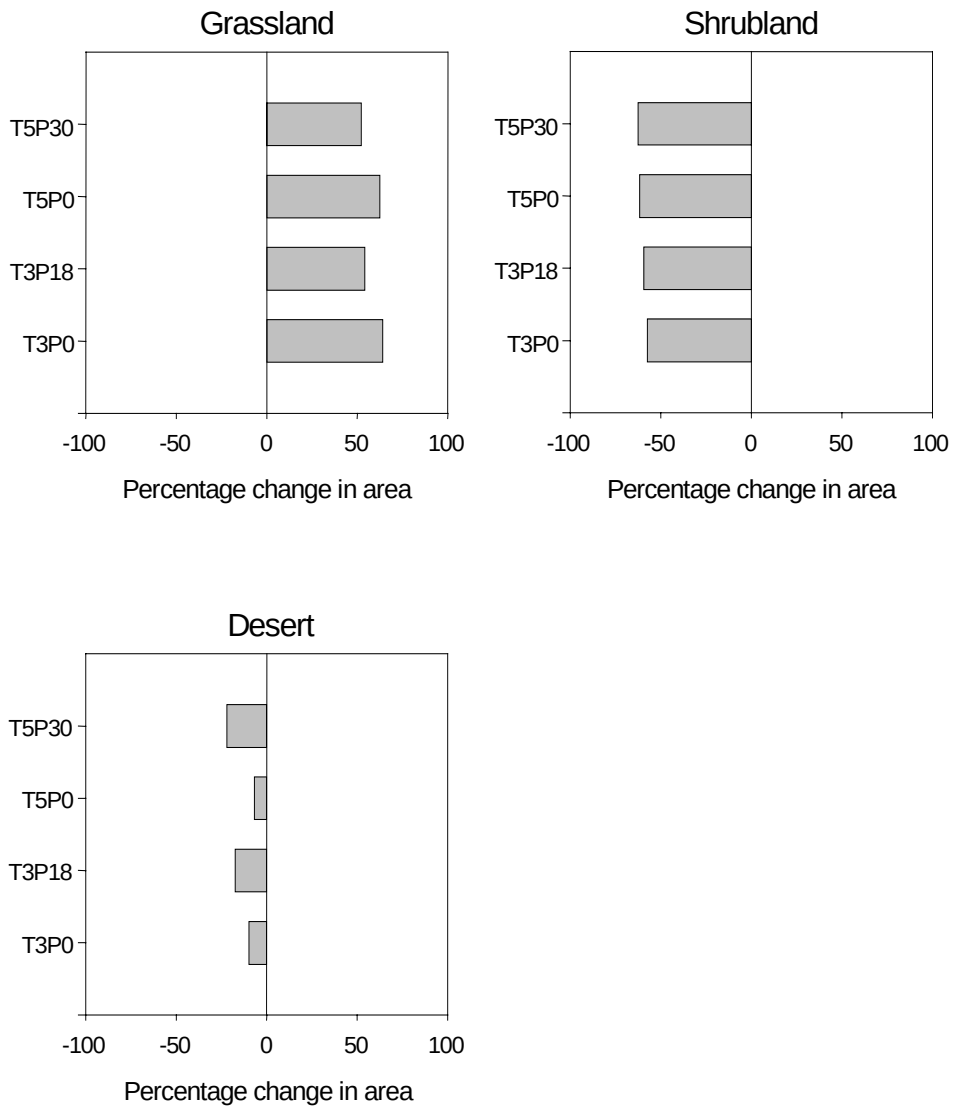

Figure A.4 (cont.). Percent changes in the simulated total cover of the vegetation classes under the incremental climate scenarios. Changes were calculated for the 30 year future period (2070-2099) relative to the historical period (1961-1990).

The common response of the vegetation classes under all four incremental scenarios was an increase in the total coverage of mixed evergreen forest and grassland classes and a decrease in the coverage of the other five classes. The mixed evergreen forest responded to the warmer temperatures by advancing into the historical range of evergreen conifer forest. This response to temperature was the result of a widespread change in the simulated life form composition from needleleaf dominance to mixed needleleaf-broadleaf in the northern half of the state. Mixed evergreen forest also responded to the wetter scenarios (T3P18 and T5P30) by advancing into the historical range of mixed evergreen woodland. This response to increased precipitation was prompted by an increase in carbon density at the ecotone between these two classes.

Grassland responded to the drier scenarios (T3P0 and T5P0) by advancing into the mixed evergreen woodland and shrubland classes. The decrease in effective moisture favored grass over woody lifeforms at the ecotones between grassland and these two vegetation classes. Grassland responded to the wetter scenarios (T3P18 and T5P30) by advancing into desert. Increased available moisture at the ecotone between these two classes prompted increases in both grass and woody carbon density. The increase in total vegetation biomass produced more fuel and fire, which favored the expansion of grassland.

Losses in the coverage of evergreen conifer forest to the advancement of mixed evergreen forest under all incremental scenarios were partially counterbalanced by gains in the Modoc Plateau and eastern Sierra Nevada bioregions. Here warmer and especially wetter conditions prompted an increase in woody carbon density and a resultant expansion of evergreen conifer forest into woodland and shrubland. The net result of this retreat and advancement of evergreen conifer forest ranged from nearly no change in coverage under the most cool and wet scenario (T3P18) to the greatest decrease under the most warm and dry scenario (T5P0).

Mixed evergreen woodland and shrubland responded with nearly uniform losses of coverage under all the incremental scenarios. Losses under the drier scenarios (T3P0 and T5P0) were mostly to the advancement of grassland; losses under the wetter scenarios (T3P18 and T5P30) were typically to the advancement of the mixed evergreen and evergreen conifer forest classes.

The losses in coverage of the desert class under all the incremental scenarios were to advancements in grassland. Under the drier scenarios (T3P0 and T5P0), these losses were relatively small and confined to the southern end of the Great Central Valley where the frequency of grassland and desert classes where nearly equal in the last 30 years of the future simulation period. Under the wetter scenarios (T3P18 and T5P30), desert suffered relatively greater losses to grassland in the southern central valley and within the Mojave and Sonoran Desert bioregions.

The losses in coverage of the alpine/subalpine class to advancement of evergreen conifer forest and shrubland were predominately a response to a longer growing season brought on by the warmer temperatures, and were most pronounced under the warmest scenarios (T5P0 and T5P30).

A.3 Response of Carbon Density and Net Biological Production to Incremental Scenarios

The response of carbon density under the incremental scenarios was determined by comparing the simulated statewide total density in different carbon pools averaged over the 30 year historical period (1961-1990) against the same averaged over the last 30 years (2071-2100) of the incremental scenarios (Table A.2). Trends in net biological production over the entire 100 year future period were also examined (Figures A.5 and A.6).

There was an increase over historical levels in average total ecosystem carbon density during the last 30 years under all four incremental scenarios. The increase ranged from 2.7% under the relatively warm and dry scenario (T5P0) to 5.2% under the relatively cool and wet scenario (T3P18). These increases were caused to a large extent by changes in soil and litter carbon, which showed the greatest increase under the relatively cool scenarios (T3), and significantly less increase under the relatively warm scenarios (T5). The response of the soil and litter pool to changes in precipitation was relatively slight, suggesting the main response of this pool under the different incremental scenarios involved temperature-mediated changes in the rates of decomposition.

Table A.2. Simulated total carbon density for the state in different carbon pools averaged over the 1961-1990 historical period, and percentage changes in the different pools under the incremental scenarios

	HIST	T3 change (%)		T5 change (%)	
Carbon pool	**(Tg)**	**P0**	**P18**	**P0**	**P30**
Total ecosystem	5765	+4.8	+5.2	+2.7	+3.5
Soil and litter	5305	+4.6	+4.7	+2.7	+2.9
Total live vegetation	461	+6.5	+10.6	+2.8	+10.0
Live wood	300	-3.7	+3.3	-8.3	+4.7
Live grass	163	+25.8	+23.9	+23.3	+20.3

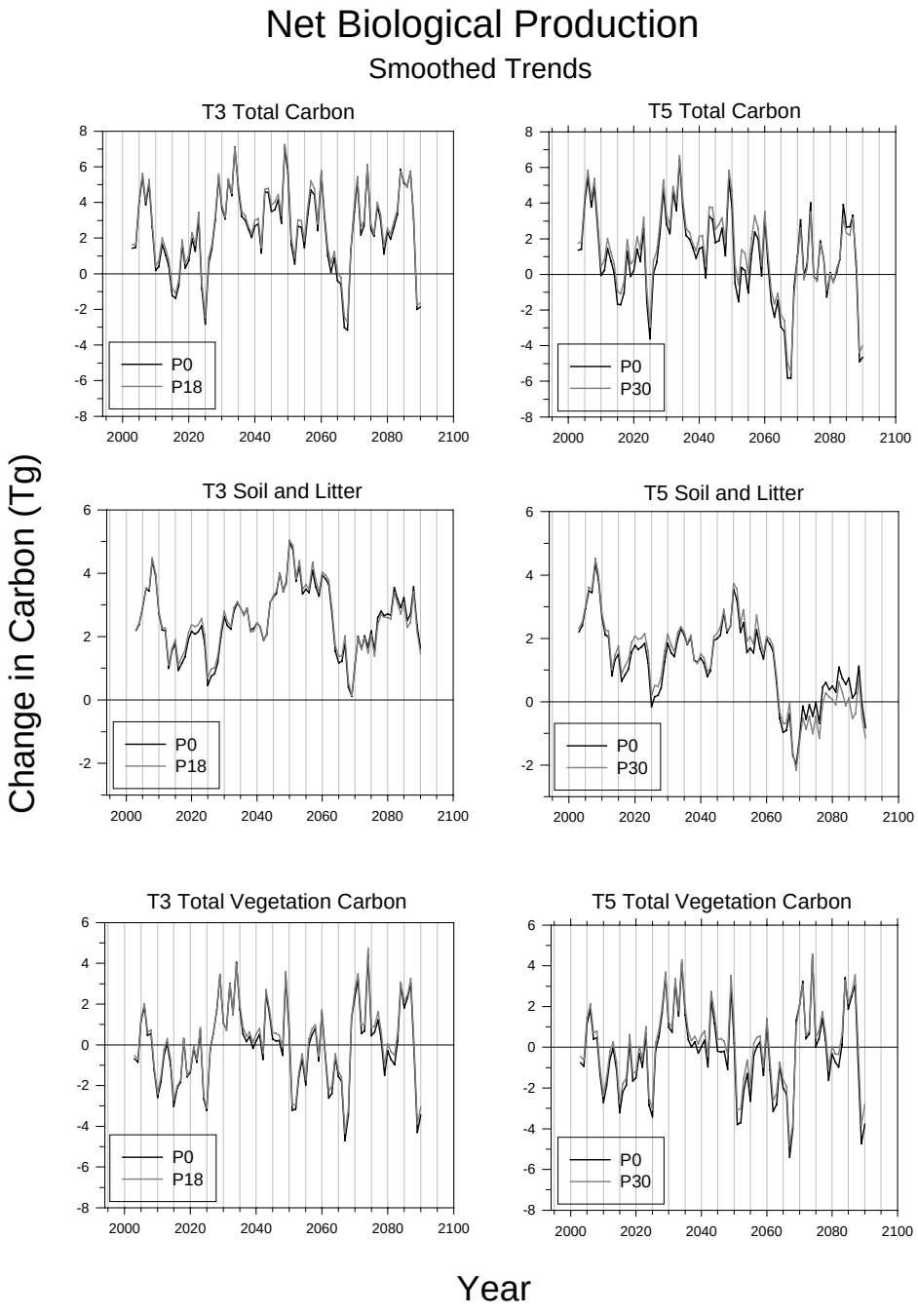

Figure A.5. Simulated net biological production (NBP) of total ecosystem, soil/litter, and vegetation carbon under incremental climate scenarios. NBP was calculated as the year-to-year change in carbon density. Trends were smoothed for display using a 10 year running average.

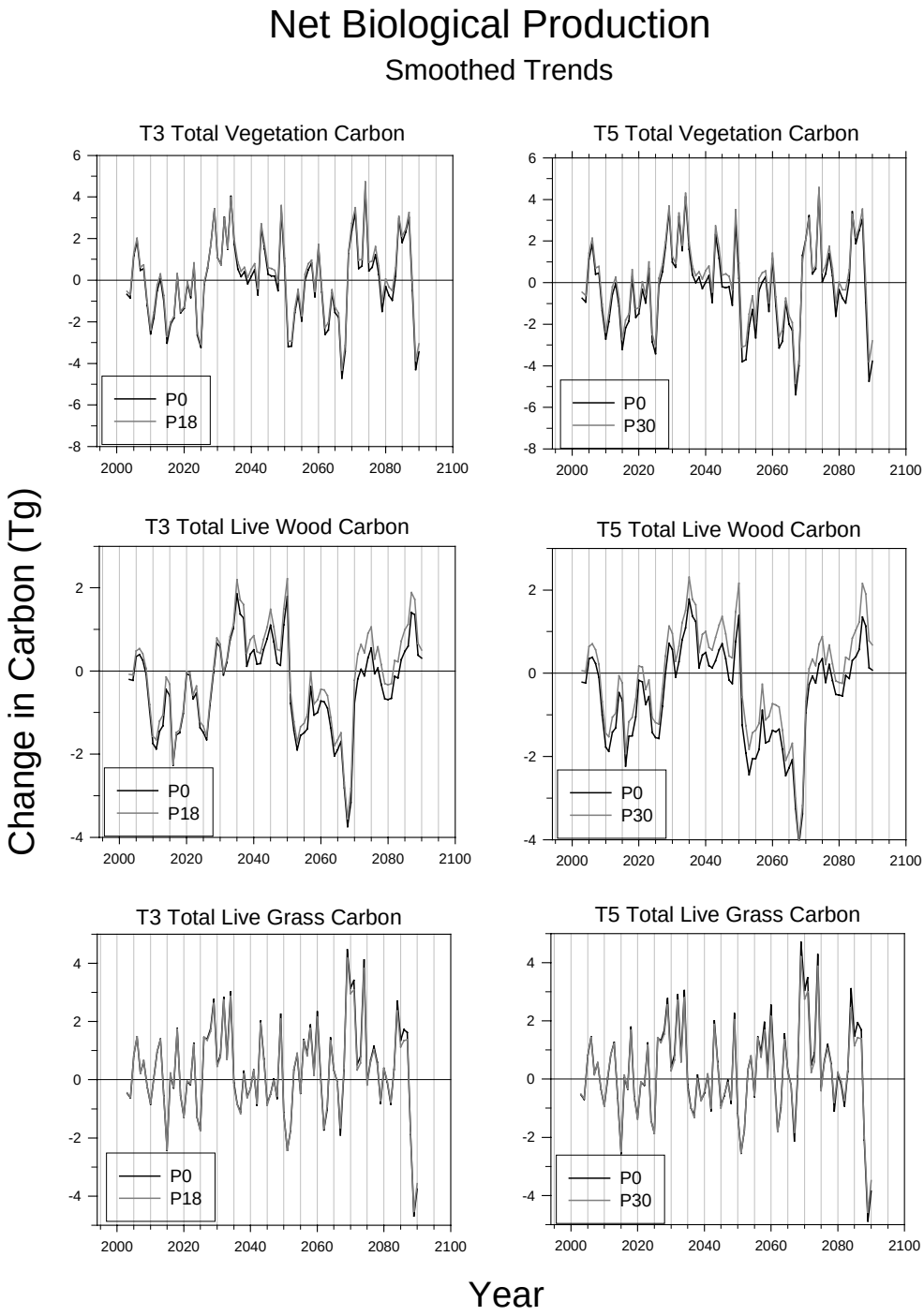

Figure A.6. Simulated NBP of total vegetation, woody, and grass carbon under incremental climate scenarios. NBP was calculated as the year-to-year change in carbon density. Trends were smoothed for display using a 10 year running average.

An increase over historical levels in average total live vegetation density during the last 30 years was seen under all four incremental scenarios. This increase was especially pronounced under the two wetter scenarios (T3P18 and T5P30), where there were increases in both wood and grass carbon density. Declines in live wood carbon density under the drier scenarios (T3P0 and T5P0) were partially counterbalanced by even greater increases in grass carbon density, thus producing relatively small net gains in the total live vegetation pool under these two scenarios.

In summary, gains in total ecosystem carbon under all four incremental scenarios were the net result of gains in vegetation carbon density that more than compensated for losses associated with temperature-driven increases in the rates of soil and litter decomposition. Gains in live vegetation carbon density were a response to both increases and declines in effective moisture. Relatively small net gains in vegetation carbon were maintained even with declines in effective moisture via simulated shifts in life form dominance toward the more drought-tolerant grasses.

Although the results show an average increase in carbon density relative to historical levels during the last few decades of the future period, trends in NBP of the ecosystem over the entire 100 years show that there were earlier periods when the simulated ecosystem was a source, not a sink, for carbon under all four incremental scenarios (Figures A.5 and A.6). These periods of decline in NBP are coincident with declines in the trend of total annual precipitation. Coupled with continued increases in mean annual temperature, these declines in effective moisture reduced vegetation productivity (and especially woody vegetation productivity). Subsequent reductions in live vegetation turnover to the soil and litter carbon pool, together with increasing rates of decomposition with higher temperatures and losses of carbon stocks to fire, resulted in a net decline in total ecosystem productivity during these relatively dry periods.

A.4 Response of Fire to Incremental Scenarios

The simulated annual area of the state burned increased under all four incremental scenarios (Figure A.7). The overall trend in the increase showed a strong relationship to the trend in increasing temperature. Peaks along the trend line are associated with relatively low annual precipitation and relatively high vegetation productivity (i.e., available fuel) in preceding years. The relationship between area burned and vegetation productivity is also demonstrated by the slightly higher levels of total annual area burned under the wetter scenario at each level of temperature increase. Vegetation productivity was somewhat greater under each wetter scenario (Figure A.6).

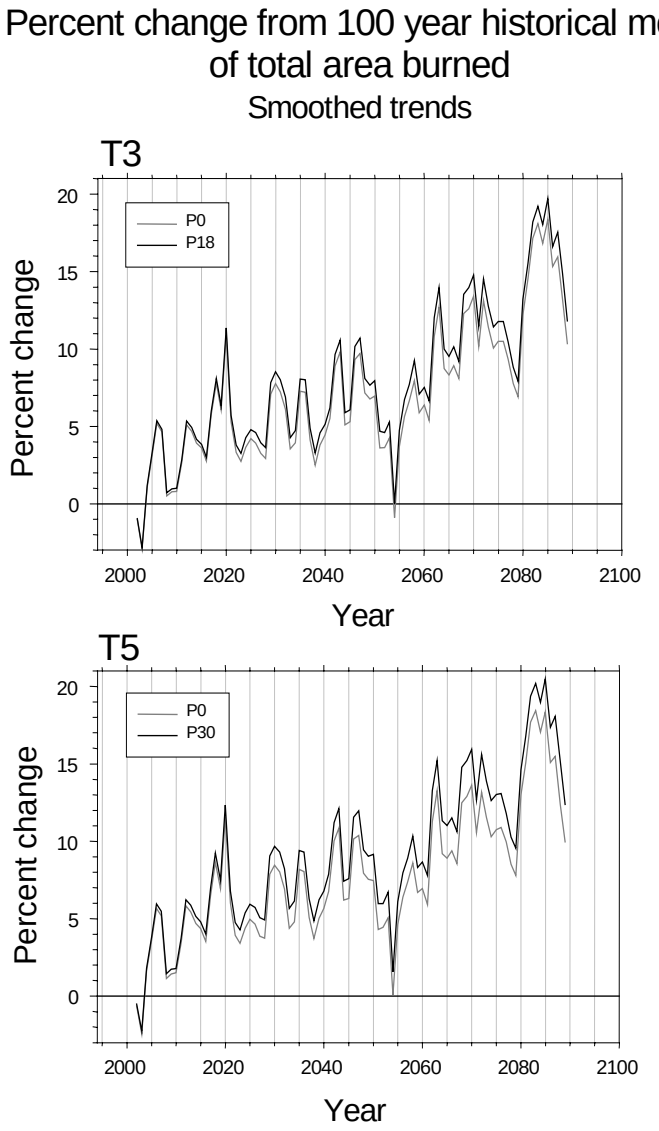

Figure A.7. Percent changes in annual total area burned relative to the 100 year historical mean under the T3 and T5 scenarios. Trends were smoothed for display using a 10 year running average.

A.5 Carbon Dioxide Response Functions in MC1

MC1 responds to increasing atmospheric CO_2 with (1) a simulated increase in maximum potential production, and (2) a simulated decrease in the rate of transpiration (thus reducing water stress). Multipliers are calculated as a function of input data specifying the atmospheric CO_2 concentration at the current timestep of the model. These multipliers are then applied to the simulated production and transpiration rates.

Although there is good evidence for short-term increases in the rates of photosynthesis and tree growth with increased CO_2, evidence for the sustainability of the response is more limited (Aber et al., 2001). Some longer term studies suggest that an accumulation of photosynthetic reserves may lead to the down-regulation (i.e., reduction) of photosynthetic rates over time. Other studies have shown no convincing evidence for down-regulation. Other limiting factors (e.g., nutrients, water, and light) could also place constraints on the direct response to increased CO_2. There is also uncertainty whether stomatal conductance, and thus transpiration, is reduced under elevated CO_2 (Aber et al., 2001). However, increased water use efficiency (the ultimate result of reduced transpiration in the model simulations) will likely increase with or without changes in conductance simply because of the greater availability of atmospheric CO_2.

Given that there may be insufficient information to support a generalized prediction of the direct to elevated CO_2, additional model simulations were generated for California under the assumption of no change in atmospheric CO_2 (from a constant concentration of 295 ppm) to gauge the magnitude of the simulated CO_2 effect with time. Table A.3 compares the mass of the total live vegetation carbon pool simulated under the no change assumption to that simulated under the assumption of increasing CO_2. The results show a 4% increase in the mass of the carbon pool at the end of the historical period because of the simulated CO_2 effect. The magnitude of the effect increases with increasing CO_2 up to 11% and 14% by the end of the future period under the HadCM2 and PCM scenarios, respectively. The larger percentage increase in vegetation carbon resulting from the CO_2 effect under the PCM scenario can be attributed to the benefit of increased water use efficiency under this significantly drier future climate scenario.

Table A.3. Mean weight (Tg) of simulated total live vegetation pool for California, with and without the CO_2 effect, for the baseline historical (1961-1990) period and 30 year future period (2070-2099) of the HadCM2 and PCM climate scenarios

	Total live vegetation carbon (Tg)	
Scenario	**With CO_2 effect**	**Without CO_2 effect**
HIST	461	445
HadCM2	568	514
PCM	539	473